Available online at www.sciencedirect.com

ScienceDirect

journal homepage: www.elsevier.com/locate/he

Review Article

Research and demonstration on hydrogen compatibility of pipelines: a review of current status and challenges

Hantong Wang [a], Zhi Tong [a], Guijuan Zhou [a], Ci Zhang [a], Hongyu Zhou [a], Yao Wang [b], Wenyue Zheng [a,*]

[a] National Center for Materials Service Safety, University of Science and Technology Beijing, Beijing 100083, China
[b] South China Company of National Petroleum and Natural Gas Pipe Network Group, Guangzhou 510620, China

HIGHLIGHTS

- Summarized projects of pure-hydrogen and natural gas-hydrogen blending pipelines.
- Discussed the factors affecting hydrogen compatibility of pipeline.
- Reviewed the testing methods for assessing hydrogen-steel compatibility.
- Presented a new proposal for toughness test for pipeline slow loading condition.
- Several challenges facing the high-pressure hydrogen pipelines are outlined.

GRAPHICAL ABSTRACT

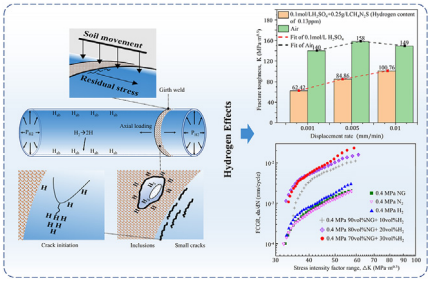

ARTICLE INFO

Article history:
Received 27 April 2022
Received in revised form
14 June 2022
Accepted 17 June 2022
Available online 10 July 2022

Keywords:
Hydrogen embrittlement
Demonstration projects

ABSTRACT

Hydrogen transportation by pipelines gradually becomes a critical engineering route in the worldwide adaptation of hydrogen as a form of clean energy. However, due to the hydrogen embrittlement effect, the compatibility of linepipe steels and associated welds with hydrogen is a major concern when designing hydrogen-carrying pipelines. When hydrogen enters the steels, their ductility, fracture resistance, and fatigue properties can be adversely altered. This paper reviews the status of several demonstration projects for natural gas-hydrogen blending and pure hydrogen transportation, the pipeline materials used and their operating parameters. This paper also compares the current standards of materials specifications for hydrogen pipeline systems from different parts of the world. The hydrogen compatibility and tolerance of varying grades of linepipe steels and the relevant

* Corresponding author.
E-mail address: zheng_wenyue@ustb.edu.cn (W. Zheng).
https://doi.org/10.1016/j.ijhydene.2022.06.158
0360-3199/© 2022 Hydrogen Energy Publications LLC. Published by Elsevier Ltd. All rights reserved.

Hydrogen compatibility
Steel microstructure
Fracture toughness
Fatigue crack growth rate

testing methods for assessing the compatibility are then discussed, and the conservatism or the inadequacies of the test conditions of the current standards are pointed out for future improvement.

© 2022 Hydrogen Energy Publications LLC. Published by Elsevier Ltd. All rights reserved.

Contents

Introduction

CO_2 emission is a major contributing factor to global warming, so fossil fuels are being replaced by clean energy sources such as hydrogen fuels. Hydrogen plays a 'carrier role' in converting wind, hydro, solar energy, and other renewable sources into the energy consumed by the end-users. China is now scaling up the development of hydrogen energy in its effort to achieve carbon neutrality before Year 2060.

The various ways of producing hydrogen are shown in Table 1, along with the economics and emission reduction matrix. The production from renewable sources has demonstrated a decisive advantage in terms of CO_2 emission and capital return [1]. For China, which imports the majority of its natural gas, hydrogen production from methane conversion can lead to a shortage of fossil fuel reserves.

Power-to-Gas technology (P2G) is a process in which the energy generated by solar and wind is turned into hydrogen and is delivered to the demand side in the form of hydrogen gas. The P2G solves the problems associated with load stability issues of power transmission lines and the difficulty of large-scale electricity storage [2–5]. Fig. 1 illustrates the process of P2G hydrogen application [1], which consists mainly of hydrogen production, transportation, and end-use. The key features of P2G include:

- Energy storage: the compressed or liquefied hydrogen pumped to underground or aboveground vessels and pipes.

Table 1 – Economic and emission assessment of different ways of hydrogen production [1].

No.	Assessment / Method	H_2 output (t/y)	Capital costs ($1m)	CO_2/H_2 (t/t)	H_2 costs ($/t*y)	CO_2 emission (g/MJ)	Profits ($1m)	Capital return (%)	Emission reductions [t/$1m/y]
1	Turbines +Inventys CCUS+ Electrolysis	22664	445	32.7	19634	109	38.5	9.1	-116
2	Fuel cell +Inventys CCUS + Electrolysis	22664	734	27.3	32386	89	40.3	5.8	4
3	Renewable energy electrolysis, 0.05 dollars/kWh	22664	130	0.4	5736	3.3	83.3	77.5	1816
4	Renewable energy electrolysis, 0.02 dollars/kWh	22664	130	0.4	5736	3.3	149	136	1816
5	Turbines +Inventys CCUS + Steam methane reforming (SMR)	22664	214	11.7	9442	48.5	131.8	62	528
6	Turbines +Inventys CCUS + Combustion oxygen SMR+ Electrolysis	25497	272	15.9	10668	30	176.7	65.8	675
7	Turbines +Inventys CCUS + Methane decomposition	22664	182	3.5	8030	29.7	216.1	119.6	897

CCUS: Carbon Capture, Utilization and Storage; Shades of green indicate environmentally friendly options; Shades of brown indicate polluting options; Brightness indicates the degree of environmental protection or pollution; Rows 3 and 4 indicate the cost of power generation in areas with average level and abundant wind resources, respectively.

- Combustion: the natural gas-hydrogen blending or pure hydrogen, could be utilized as the fuel gas in order to replace the natural gas for home heating and combustion.
- Power generation: the gas turbine provides electricity by burning blended hydrogen gas or even pure hydrogen gas. The adaptation of hydrogen generation technologies can provide a safer end-use environment, as electricity delivery is much safer than hydrogen delivery to the homes of the mass population.

Safe and economical hydrogen delivery is an essential part of P2G, and thus hydrogen pipelines play an essential role in the development process of renewable power utilization and decarbonization. Trucking and pipelines are the main ways to transport gaseous hydrogen, and pipeline delivery is more economical, especially in the case of large-scale, long-distance transport [5] [–] [8]. The International Energy Agency (IEA) reported in 2019 that local distribution by trucks was an economical method for deliveries of distances of less than 500 km. If the distance is more than 500 km, then pipeline becomes more cost-efficient and environmentally sound in delivering hydrogen than other means [9]. Other potential delivery methods are also being developed, such as liquid hydrogen, liquid ammonia, and liquid organic hydrogen carriers (LOHCs). However, they invariably involve additional processing steps (such as gas to liquid conversion) in achieving the final gaseous state of hydrogen fuel.

In addition to economics, the usage of pipelines for hydrogen transportation alleviates the problem of the imbalanced distribution of renewable sources. For example, the western part of China is abundant in renewable energy, but the energy demand is mainly concentrated in the eastern region, and the 'surplus power' in the west cannot be supplied directly to the east via the high voltage power grid at the moment due to either the availability or the stability issue of the power grid [4]. Therefore, pipeline is a good alternative to ship this green energy from the west to the east part of China. Obara [3] evaluated the economic and environmental benefits of hydrogen transportation via the existing natural gas pipeline from Qinghai province to Shanghai city of China. With a 42.4% overall efficiency of the Qinghai-Shanghai system, which is based on the electricity obtained from photovoltaics in Qinghai, emission reduction of this large-scale project would amount to 3.02 Gt of CO_2, 104 kt of SO_x, and 134 kt of NO_x.

It is widely known that hydrogen in steel can increase the failure probability of the material due to hydrogen embrittlement [10,11]. When hydrogen enters the steel, their mechanical properties, fracture resistance, and fatigue growth rates can be adversely affected. The growth of defects from pre-existing flaws of in-service pipelines will also be accelerated by hydrogen. The hydrogen compatibility of pipeline steel is an issue of common interest. Assessment of this compatibility means evaluation of the mechanical properties of a steel in the hydrogen environment or with hydrogen-charging under its expected loading conditions in consideration of its design life, and there have been reviews of specific aspects related to this compatibility issue.

Dwivedi [12] reviewed the failure mechanisms and characterization methods of hydrogen embrittlement in different high-strength steels, and discussed mostly the use of coating

techniques to prevent hydrogen embrittlement; Ohaeri [13] provided an overview of hydrogen damage mechanisms for pipeline steels, and suggested that microbial activities can also exacerbate the effects on hydrogen embrittlement for pipeline steels; The problem of hydrogen cracking in girth welds is recently summarized by Sun [14]; and Xia et al. [15] discussed the synergistic effect of multiple mechanisms in hydrogen embrittlement, and reviewed the experimental methods for the study of diffusion kinetics of hydrogen. The authors concluded that the compatibility tests in gaseous hydrogen are more applicable to actual working environment. Although many studies have focused on the resistance to hydrogen embrittlement of pipeline steel, there remains a need to link these studies to the actual operational requirements of pipeline steel in a pressurized hydrogen environment. In making such linkage one needs to be aware of gaps that exist in test conditions or analytical approaches used by researchers and the actual service conditions of a complex pipeline system.

The main objective of this article is to clarify the key factors that influences the hydrogen-steel compatibility in view of the large range of loading conditions of pipeline systems and of the complexity of the metallurgical characteristics of steels involved, and assess the tolerance of different grades of pipeline steels to hydrogen. To fulfill this goal, we have investigated the current status of domestic and international hydrogen pipelines, reviewed the studies on the tensile properties, fracture resistance and fatigue crack growth rates of various pipeline steels in different hydrogen-containing environments, and then discussed, in particular, the effect of loading rate or loading frequency on compatibility testing results. In this process we have identified the conservatism or inadequacy of current standards, which we have pointed out in this paper for future improvement.

Demonstration projects of hydrogen pipelines

International demonstration projects

Before natural gas was widely used, coal gas (a.k.a. Town Gas) was utilized in the cities and towns of America. The gas may contain up to 50% hydrogen and about 5% carbon monoxide, the delivery pressure was as low as about 2 MPa [10]. A long-distance hydrogen pipeline of 215 km was first built in Ruhr, Germany, in 1938, with a diameter between 168 and 273 mm, an operating pressure of less than 2.5 MPa and 10^6 m^3/year of delivery capacity [16]. Currently, the total length of the European hydrogen pipeline is reported to be over 1600 km, of which the longest one (1103 km distance) is operated by Air Liquid [11]. This particular long-distance hydrogen pipeline runs from northern France and Belgium to the southwest of the Netherlands, with an average pipe diameter of 168 mm. At the same time, the pressure reaches as high as 10 MPa [17].

Pure hydrogen pipeline now exceeded 2500 km in the USA, where Air Products have been operating the longest hydrogen pipeline from Texas to Louisiana at over 983 km. It is almost entirely made of low carbon steel, including vintage ASTM 106 and API 5L Grade B steel, as well as the modern API 5L X42/X52 steel, of up to 360 mm diameter and operating pressures ranging from 3 to 5 MPa. This pipeline network supplies pure hydrogen to the refineries and chemical factories along the Texas Gulf Coast [16].

A hydrogen pipeline of approximately 18 km in Southern California is completely made of low-strength steel, typically API 5L Grade B and some of API 5L X42, with a diameter of 200–300 mm and a thickness of 4.5–8.6 mm, operating at 3.5–6.2 MPa pressure. It is worth noting that a short X52 pipeline near the city of Carson is now working at high pressures of up to 14 MPa [18]. The detailed features of some of the demonstration projects in the EU and US are reproduced in Table 2.

Table 3 summarizes the demonstration projects for the hydrogen-nature gas blend. The NaturalHy project showed the feasibility and the risks of blending hydrogen, the results showed no separation phenomenon of mixture gas inside the pipes occurred; In addition, the blended natural gas with less than 20% hydrogen showed a similar severity in terms of explosion impact to that of natural gas. NaturalHy also found a higher individual risk (person fatality) when increasing hydrogen concentration over this limit [21]. NaturalHy mainly applied polyethylene (PE) and polyvinyl chloride (PVC) pipes in order to test the hydrogen compatibility in the natural gas distribution system. However, the blending ratio was limited

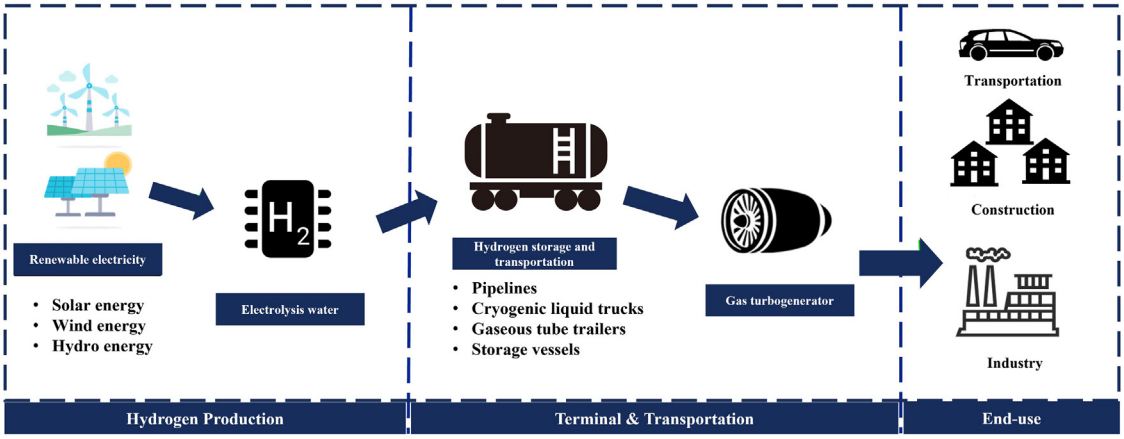

Fig. 1 – Schematic of P2G energy conversion process [1].

Table 2 – Summary features of some pure hydrogen pipelines in the EU and US [11,16,18] [–] [20].

Project name	Materials	Diameter (mm)	Pressure (MPa)	Distance (km)	Country	Start-up of operation
Air Liquide, Chemische Werke	SAE 1060[a]	168–273	< 2.5	215	German	1938
Air Liquide	Seamless Carbon steel	158	< 10	> 1100	France-Netherlands	1966
Air Products, Texas-Louisiana	Varies[b]	76–356	3–5	> 983	USA	Before 1999
Air Products, Southern California	API 5L Gragde B	168–323	3.7–6.2	18	USA	2010
New Air Products Carson Plant	API 5L X52	219	14	0.9	USA	NEW

[a] Similar to API 5L X46.
[b] Include ASTM 106, API 5L Grade B/X42/X52.

Table 3 – The demonstration project of natural-gas and hydrogen blending.

Project name	Objective	Blending ratio	Country	Start end up
Naturalhy [22,23]	Feasibility evaluation	< 20%	EU	2002–2006
Ameland [24]	Testing of end-users in community	12%	Netherlands	2004–2009
WindGas Falkenhagen [30]	Demo P2G integration technology	10%	Germany	2012
Energiepark Mainz [25]	Development, testing and application of P2G	0–15%	Germany	2013–2016
GRHYD [31]	Development, testing and application of P2G	20%	France	2018
HyDeploy [26]	Demonstration of burning hydrogen in homes	0–20%	Britain	2018
SNAM [27]	Improving the hydrogen content of injection by pipeline	10%	Italy	2019
Hydrogen Park-SA [32]	Development, testing and application of P2G	5%	Australia	2019

to 20% of hydrogen, and the pressure tolerance is only 0.6 MPa (Maximum Allowable Working Pressure) for such pipes. It concluded that polymer materials are compatible with hydrogen at the pressures involved. This is because hydrogen cannot provide the chemical radicals that can induce damage in the molecules of the polymer materials. In addition, NaturalHy also concluded that, at the operating pressures (lower than 1.72 MPa) and stresses level (less than 20% SMYS) of the distribution system, metal pipes (grade level less than X46) would not fail in a brittle model, but may show loss of partial ductility [22,23].

A 75 mm PVC pipe was used in the Ameland project to deliver 30% hydrogen and 70% natural gas within a community, and it validated the findings of Naturalhy on the suitability of PVC materials [24]. Energiepark Mainz project delivered up to 15% of the hydrogen to the natural gas pipe network but operated at less than 1 MPa pressure [25]. HyDeploy demonstration project indicated that the plastic pipes were not degraded with hydrogen up to 20% and 0.05 MPa pressure, and blended hydrogen can be safely burned without changes in the home appliances [26]. The Italian company SNAM operated the Contursi Terme blend gas network with 10% hydrogen, and a capacity of 70×10^9 m^3/year, and reported that more than 20,000 km of hydrogen pipelines could be ready for blend gas delivery [27].

Although several projects verified the feasibility of blending hydrogen in the gas distribution system, it is not clear whether hydrogen is compatible with the material for long-term service. The main objective of the HyBlend team was to assess hydrogen compatibility with pipeline materials for improving the blending ratios and quantifying the costs and possibilities of blending hydrogen [28]. Hydrogen Materials Compatibility (H-Mat) consortium built a technical database for research on hydrogen-materials compatibility, the data contained the effect of hydrogen on the mechanical properties of the material, the interactions of microstructure and hydrogen, and the behavior of hydrogen absorption, diffusion and trapping [29].

The polymer pipes are widely used in the distribution system, and the data showed that the working pressure was typically lower than 0.69 MPa, with diameters between 120 and 200 mm or less [21]. Hydrogen permeability through the polymer pipe is a potential concern, especially in the enclosed space. NaturalHy [33] found that hydrogen permeability is about five times higher than that of methane in PE pipes, and the permeability increases with pressure. NaturalHy also demonstrated that the aging of PE pipes did not affect hydrogen diffusion. Haines [34] estimated the loss of hydrogen leakage at a negligible 0.00005% of the annual delivery volume with 17% hydrogen injection. It is worth noting that the contaminants may cause deterioration inside pipes, and the risk of leakage in the welding region of the polyethylene is an unsafety issue to consider [35]. In summary, hydrogen has no significant degradation on PE materials, but strength, stiffness, and pressure-bearing capacity of plastic pipes are much less than steel pipes and are not suitable for transporting high-pressure hydrogen.

However, there are hardly any reports of demonstration projects for blending hydrogen transportation at high pressure. According to the U.S. DRIVE investigation (United States Driving Research and Innovation for Vehicle efficiency and Energy sustainability) [36]. One key characteristic of existing gas pipelines is that there exist numerous small defects in the pipe and pipe welds, as a result of service damage or manufacturing deficiencies. The minor cracks were hard to detect, yet when there is hydrogen present, existing defects could quickly grow to critical size then fracture at high pressure or high axial loading.

Table 4 – Summary of key features of pure hydrogen transportation in China.

Project name	D(mm)	P(MPa)	Material	t(mm)	L(km)	F
JinLing-YangZi	325	4	20# seamless steel	12	32	0.22
BaLing-ChangLin	406	3.5	20# seamless steel	10	42	0.29
JiYuan-LuoYang	508	4	L245 seamless steel	N/A	25	N/A
WuHai-YinChuan[a]	610	3	L245 LSAW	8–12.5	217.5	0.3–0.47
YiMa-ZhengZhou[a]	426	2.5	SM400C SSAW	N/A	194	N/A
DingZhou-GaoPi[b]	508	4	L245-L360	10–14	145	0.2–0.41

LSAW: Longitudinally Submerged Arc Welding; SSAW: Spirally Submerged Arc Welding; Where D is the outer diameter of pipeline, P is the design pressure, t is the pipeline wall thickness, F is the design factor where the welding parameters and temperature de-rating factor assume to be 1.0.

[a] Coke oven gas pipes.

[b] In planning and construction.

The long-distance nature gas pipeline in the USA was usually made of medium-to-high grades pipeline steel, which operates at high pressures up to about 14 MPa. Furthermore, the operating stress of Class I pipelines was designed up to 80% of the specified minimum yield strength (SMYS) [21,36]. It would be challenging to operate hydrogen pipelines at such high pressure. To address the safety of high-pressure hydrogen transport, US DOE set up a unique project to develop fiber-reinforced polymer pipelines (FRP) in the USA. FRP is mainly covered with high-density polyethylene (HDPE) inside for preventing hydrogen permeation, which is available up to 300 mm diameter and 6.8 MPa pressure rating. Moreover, the FRP could be produced on-site with a length of up to 4.8 km, significantly reducing the cost of welding and transporting by about 25% [36].

Demonstration projects in China

Table 4 provides details of the projects of pure hydrogen pipelines in China. They are all made of seamless and low-grade pipes (20# and L245), and the design pressure is below 4 MPa, since safety concern is of primary importance in the projects. The design factors shown as F in Table 4, are typically around 0.3, which is conservative in terms of safety consideration. These pipelines mainly transport hydrogen to petrochemical companies for use as chemical raw materials.

The 20# and L245 steels have good plasticity, toughness, and welding properties. In all these hydrogen projects, the joining of pipe sections was performed by manual welding. Sometimes the quality of manual welding is influenced by random factors, including out-of-range welding parameters, resulting in poor weld quality and even small cracks. According to some reported failure cases [37] for L245 and 20# natural gas pipelines, brittle fracture failure is mainly caused by these cracks and minor defects, especially at girth welds. Moreover, for the pipe bend and tee joints, improper control of the forming process and heat treatment is also prone to generating cracks [38]. In some of the steels, inclusion interfaces, ferrite and M-A island interfaces, and grain boundaries with M-A islands become a vital site where cracking can easily nucleate and expand.

Overall, plastic pipes (PVC or PE) are compatible with hydrogen, but hydrogen leakage through the joints or the valves of the piping may pose a significant risk of ignition and explosion for household applications where ventilation is insufficient. For the distribution systems that involve pressure as high as several MPa, low carbon steels are recommended for hydrogen service, e.g., as described in APL 5L PSL2 X52. However, the hydrogen compatibility of the metallic pipeline and its associated welds still needs further investigation.

Hydrogen-pipeline compatibility

Assessment of hydrogen compatibility of a pipeline materials can be performed using various testing methods, but typically includes tensile tests, slow strain rate tensile (SSRT) tests, fracture toughness, and fatigue cracking growth rates (FCGR) tests.

Hydrogen embrittlement in pipeline steels can occur by a variety of mechanisms [15,39–42], and such effects are further complicated by the presence of the residual stresses introduced by the manufacturing and welding, and by the cathodic protection on the external surface. All these factors could couple together to promote crack formation and propagation. The key factors influencing hydrogen embrittlement such as metallurgical conditions (including the steel microstructure, chemical composition, type and size of inclusions), the environment (including hydrogen concentration/pressure, gas purity), as well as by the mechanical factors such as the loading amplitude, the loading rate, frequency of these stress cycles, are discussed below.

Microstructural influences on hydrogen compatibility

Effects of grain size

The grain size of the pipeline steel is an important metallurgical factor. National Institute of Standards and Technology (NIST) [43] observed the microstructure of vintage and modern X52 steels used for hydrogen delivery, as shown in Fig. 2. NIST [43,44] found that the vintage X52 presents a higher carbon and sulfur content and larger grain size than the modern X52 and does not contain microalloying elements. The vintage X52 mainly consists of polygonal-like ferrite and pearlite, as shown in Fig. 2(a). However, Fig. 2(b) shows the new X52 was made up of irregular polygonal ferrite, acicular ferrite, and diffusible carbides. The grain sizes of vintage and modern X52 steels are approximately 24 and 13 μm, respectively. This change illustrated that grain refinement was more conducive to inhibiting hydrogen accumulation, resulting in improving

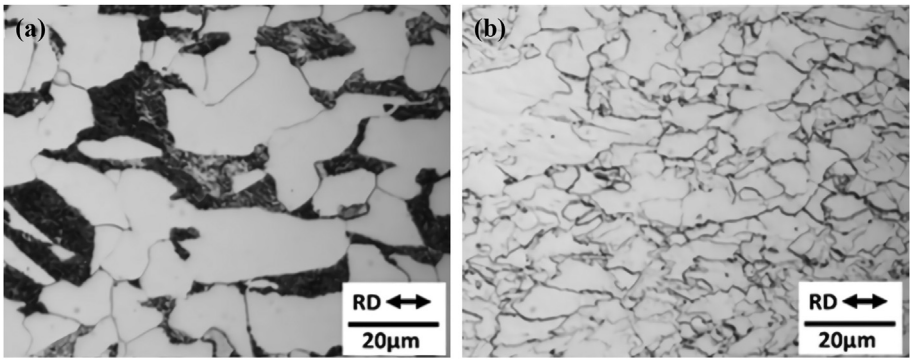

Fig. 2 – (a) Vintage hydrogen pipeline X52 with ferrite-pearlite microstructure; (b) modern hydrogen low-carbon pipeline X52 with polygonal ferrite and acicular ferrite [44].

the fracture resistance and arresting the crack propagation along the grain boundaries.

Park and co-workers [45] verified that the finer grains are beneficial in resisting hydrogen embrittlement, which was observed by in-suit slow strain rate tests on API 2W 60 steel. The specimens of refined grains gave a superior performance in the hydrogen environment. When the hydrogen is stated in terms of its amount per unit length of the grain boundary, the researchers [45] showed that fine-grained steel had a lower hydrogen concentration. Reducing grain size leads to higher in the grain boundary area, which provides more hydrogen trap sites in the grain boundary, resulting in a smaller amount of diffusible per unit length of grain boundaries than in the case of the large grain counterpart. This is true despite the fact that the fine grain material had a higher total hydrogen concentration, which was measured by the authors using the TDS technique [45].

Effects of inclusions

Inclusions of pipeline steel are mainly compounds of elements such as Al, Mn, Ca, O, S, and P, which serve as possible initiation sites of hydrogen-assisted cracking. For example, Hydrogen atoms are prone to accumulate at the tip of sulfide inclusions. Troger [46] showed that the higher sulfur content is more likely to form the MnS inclusions and produce significant segregation. While the hydrogen would not escape easily from the traps with high bonding energy, the cohesive energy of the interface between the inclusions and the matrix will drop with hydrogen accumulation at the interfaces. The inclusions also cause a large lattice distortion and thus a high local stress concentration. The accumulated hydrogen atom is able to reform into a molecules state, which will then produce hydrostatic stress around the inclusions site. In addition, the type, shape, and quantities of inclusions can highly influence the fracture resistance of hydrogen pipelines, more explanations can be found in Refs. [47–49].

The trapped hydrogen in dislocations is usually reversible due to its low-binding energy [50]. Novak et al. [51] confirmed that the severity of hydrogen-induced intergranular fracture is correlated to low-binding energy trap sites (such as moving dislocations) rather than high-binding energy trap sites such as inclusions, high-angle grain boundaries and carbide. These inclusions as the hydrogen trapping site can hinder the hydrogen diffusion. Peng [52] demonstrated that finely dispersed non-metallic inclusions in X70 steel alleviated the hydrogen effect and improved the resistance of pipeline steel to hydrogen embrittlement.

Microstructure of the girth welds

Some reported [14,53,54] that the behavior of hydrogen is different in the girth welds of various grades of pipeline. Ronevich and others [55,56] obtained a series of welded specimens of X52 to X100 by different welding process parameters, which produced welds of different strengths. After testing under a 21 MPa gaseous hydrogen, they found that the fracture toughness of these specimens was mainly correlated to the yield strength of the weld. Sun showed that the HAZ of X80 steel is the weakest site due to the hardness, strength distribution and heterogeneity structures [57]. The coarse grain heat-affected zone (CGHAZ) is the most susceptible region to cracking in the hydrogen environment due to the presence of complex and sensitive microstructures. For X80 steel, the CGHAZ consisted of granular bainite (GB) and lath bainite, where many island structures were distributed, while fine-grain heat-affected zone (FGHAZ) consists of fine acicular ferrite (AF) and polygonal ferrite (PF) [38]. Hydrogen diffuses at a higher rate in the CGHAZ than in the FGHAZ, and this is due to an reduction of the high-angle grain boundaries and

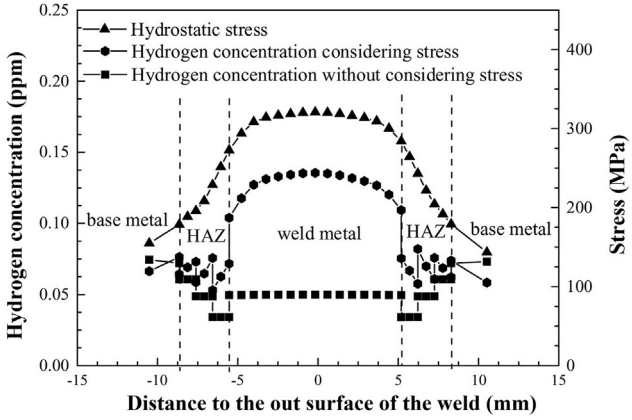

Fig. 3 – The Effect of residual stress on the distribution of hydrogen concentration in the weld area [63].

dislocation density in CGHAZ, which are able to retard the diffusion of hydrogen, and this is also observed by Zhang [58].

The M/A phases in steel and pipe welds are generated during steel production or weld solidification. Alvarez [59] demonstrated by X42 steel that the M/A phases represented a favorable site for trapping hydrogen. Xu [60] pointed out the M/A phases are the most susceptible microstructure for hydrogen-assisted cracking. The M/A phases and precipitates in steel both can trap hydrogen atoms to accelerate the void nucleation at these interfaces under tensile loading.

The residual stress in the welds

Welding also introduces additional residual stresses, which promote local hydrogen accumulation in the welds. The temperature gradient effect and thermal stresses during welding can cause localized inhomogeneous plastic deformation and phase changes at the weld region, which will lead to axial tensile residual stresses after cooling and shrinkage of the structure. Residual tensile stresses will significantly increase the risk of hydrogen cracking at the weld region [14]. The diffusion flux of hydrogen is generated by the hydrogen concentration gradient and the hydrostatic pressure gradient. The theory of increased hydrogen accumulation by stress was previously proposed by Yokobori and others [61], who explained why the distribution of hydrogen concentration is mainly influenced by the hydrostatic pressure around the crack tip. Takakuwa et al. [62] further proved that tensile residual stress force hydrogen atoms to accumulate more rapidly in high-stress areas, such as the crack tip and the elastic-plastic boundary, whereas compressive residual stress can decrease the hydrostatic pressure level for inhibiting hydrogen diffusion. Zhao and co-workers [63] analyzed the effect of residual stress on the distribution of hydrogen concentration at X80 welded joints. The authors found that, when residual stress is not considered, the level of hydrogen concentration is in an increasing order of welds metal, CGHAZ, FGHAZ, and base metal, as determined by hydrogen permeation technique. When residual stress is considered, the hydrogen concentration in the weld increases significantly, as shown in Fig. 3. Thus, it can be proven that the underlying cause of the increase in hydrogen concentration in the weld is due to residual tensile stress.

Since many factors such as pipe wall thickness, the heat input during welding, and ambient environment (e.g., humidity, temperature) will affect the distribution of residual stresses, it is not easy to calculate or measure its distribution accurately. The Fitness For Service (FFS) codes in BS 7910 and API-579-1/ASME FFS-1 [64] estimate residual stress distribution by assuming a constant value (equal to the yield strength) or by recommending an upper limit of residual stresses based on the results of simulations. The appropriate welding process parameters, inter-pass temperature, and weld filler selection are the key factors to controlling the residual stresses. After completing a weld, post-weld heat treatment and application of compressive stress (by hydro-testing, for example) are commonly used to reduce the residual tensile stress [14,65].

Assessment of tensile properties

Slow strain rate tensile test

Many studies [66–71] demonstrated that hydrogen has a negligible effect on the tensile strength, whether in a pure or blending hydrogen atmosphere. For a given class of steel, the tested yield and tensile strengths usually fluctuate somewhat, but within about 10%, as shown in Fig. 4(a). However, the loss of elongation and reduction in the area caused by hydrogen could be more than 40%. Fig. 4(b) has confirmed that the ratio of failure elongation will decrease under hydrogen influence as the yield stress of pipeline steels increases. The higher-grade pipeline steels usually show poor ductility during the SSRT. Another test on X70 steel in different hydrogen-containing environments was completed by Nguyen [72], who illustrated that the hydrogen at low concentrations (10 MPa natural gas blending with 1% v/v hydrogen) had no significant effect on tensile property of smooth specimens. Conversely, the reduction area in notched specimens with the stress concentration of a notch was significantly degraded under the same environment.

Effect of strain rate

It has been shown that dislocation movement and hydrogen diffusion has a synergistic effect in steel [73,74]. Ferreira et al. [75] observed the mobile dislocations by in-situ tensile loading during the hydrogen introduction. The results indicated that the hydrogen would weaken the pinning effect on the dislocations, promoting the movement of the dislocations. This phenomenon is because hydrogen reduces the elastic interaction force between the dislocations in the pileup, thus reducing the critical stress for emitting dislocations.

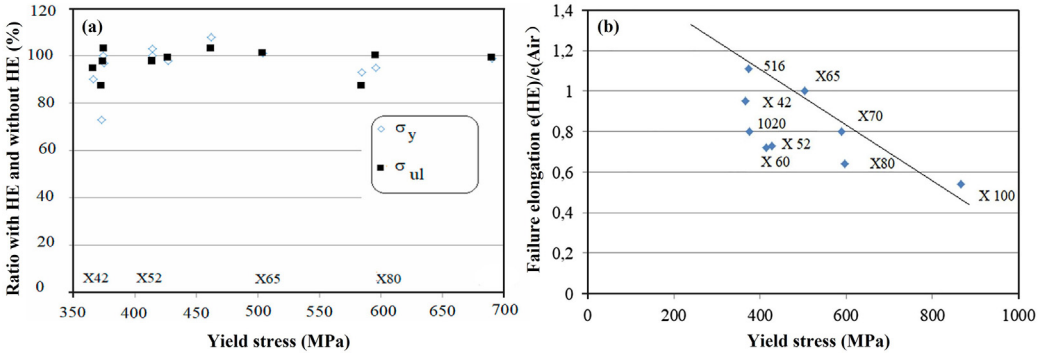

Fig. 4 – The SSRT response of different grade pipeline steels under hydrogen atmosphere [71]: (a) yield and ultimate stress; (b) failure elongation.

Therefore, when the strain rate, which governs the plastic deformation rate, is sufficiently low, the diffusion of hydrogen atoms will follow the dislocation motion. In return, the plastic strain will also lead to hydrogen accumulation. This phenomenon was also recently reported by Han [76], who evaluated the effect of pre-strain on the hydrogen embrittlement sensitivity of X100 steel. Maier et al. [77] have shown that the average hydrogen concentration is about ten times higher in dynamically loaded samples than that of samples under static loading.

The critical velocity (v_{cr}) between the movement of hydrogen and the dislocation can be determined from Tien's explanation [78], as expressed by Eq. (1). And Eq. (2) calculated the mean dislocation velocity in the tensile test using equation by Orowan [79]. The critical dislocation rate and the magnitude of the strain rate is compared by Eqs. (1) and (2) to determine whether the hydrogen can interact with the dislocation.

$$v_{cr} = D_{eff}|E_{bd}| \,/\, 30RT|b| \tag{1}$$

$$d\varepsilon \,/\, dt \approx \rho_{mob} v_D |b| \tag{2}$$

where, D_{eff} is effective diffusivity of hydrogen; |b| is Burgers vector, for X80 steel, which usually takes as 0.25 nm [79], $|E_{bd}|$ is the binding enthalpy between dislocation and hydrogen, which often take as 25 kJ/mol for X80 steel [79]; and ρ_{mob} is a density of mobile dislocation; v_D is the velocity of dislocation.

Hydrogen effects on fracture toughness

Hydrogen-induced fracture mechanism

Hydrogen can significantly decrease the ability of a material to resist crack propagation. Several plausible mechanisms can be used to explain the degradation in mechanical properties, and more detailed explanations in the hydrogen embrittlement mechanism can be found in other articles [12,15,39]. One of the most recognized models was the Hydrogen Enhanced Localized Plasticity (HELP) model, where hydrogen atoms enhance dislocation mobility, increasing plastic strain at the crack tip. This phenomenon is caused by hydrogen promoting the dislocation emission at lower stress levels, and reducing the interaction energy between dislocations, which was first proposed by Birnbaum [80]. The hydrogen can also produce a strain localization phenomenon. Hirth [81] found that the height of slips step and spacing of slip bonds will be increased with increased hydrogen concentration in low carbon and micro-alloyed steels. Thus, the strains will be concentrated in narrow slip bands. When the global strain is small, the local plastic strain may reach the yielding point, resulting in the nucleation of hydrogen-included crack.

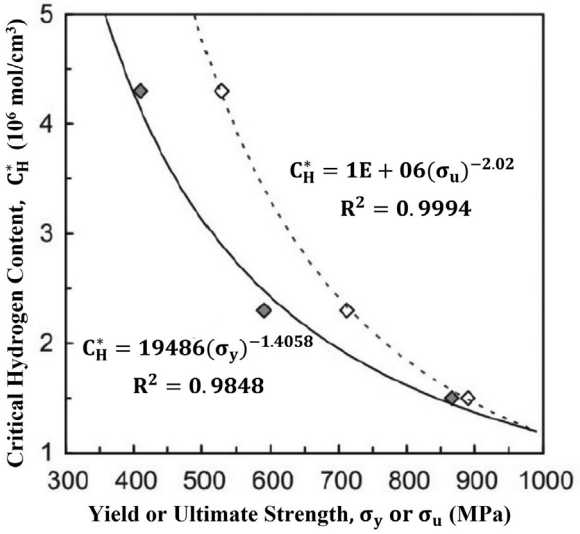

Fig. 5 – The relationship between critical hydrogen content and yield or ultimate stress in pipelines [84].

Another theory of hydrogen embrittlement is that the Hydrogen Enhanced Decohesion (HEDE) [82], where the solid solution of hydrogen atoms reduces the atomic bonding between iron atoms from σ_{th} to $\sigma_{th(H)}$ of the steel. This reduction in bonding strength is consistent with the hypothesis that hydrogen reduced surface energy γ_s of metal (based on energy change): the absorbed hydrogen can decrease the surface energy and the energy needed for plastic deformation γ_P, as described in Eq. (3). Based on experiment work by Song [83], since the surface energy is much less than the work of plastic deformation $\gamma_s \ll \gamma_{P(H)}$, the main reason for the decrease in fracture toughness K_{IC}^H or fracture stress σ_{IH} should be reflected in the plastic component of fracture energy $\gamma_{P(H)}$.

$$K_{IC}^H = \sqrt{E(2\gamma_s + \gamma_{P(H)})/1 - v^2} \tag{3}$$

where, K_{IH} is fracture toughness, E is Young's modulus, γ_s is surface energy, $\gamma_{P(H)}$ is the plastic component of fracture energy under hydrogen environment, and v is Poisson's ratio.

Capelle [84] tested the fracture energy of X52, X70 and X100 steels by means of acoustic emission techniques and defined the critical hydrogen content C_H^*. This critical value represents the hydrogen content value at which the plastic component of fracture energy significantly decreased. Fig. 5 illustrates that the critical hydrogen content tends to decrease as a power function with increasing yield strength for pipeline steels, which also verifies that high-strength steels are susceptible to hydrogen embrittlement. It can therefore be seen that the critical value of this hydrogen concentration is inversely proportional to the square of the tensile or yield strength. However, it is noted that the critical hydrogen content is also subjected to the latter include the notch size, the loading rate, and other factors.

Effects of gas impurities

The adsorption of gases on the surface causes a reduction in surface energy but does not necessarily lead to fracture. O_2, CO, SO_2, CS_2, and N_2O have been found to act as inhibitors of hydrogen embrittlement [85]. For example, Ryosuke et al. [86] & Staykov et al. [87] stated that the adsorption of carbon monoxide would mitigate the decomposition of hydrogen molecules on the surface of the base metal but would reduce the electron density of the surface layer, which results in easier migration of hydrogen atoms to the subsurface. Somerday [88] demonstrated that a minor oxygen content could inhibit hydrogen-assisted fatigue cracking in X52 steel. Ryosuke et al. [86] also illustrated the effect of O_2 on fracture

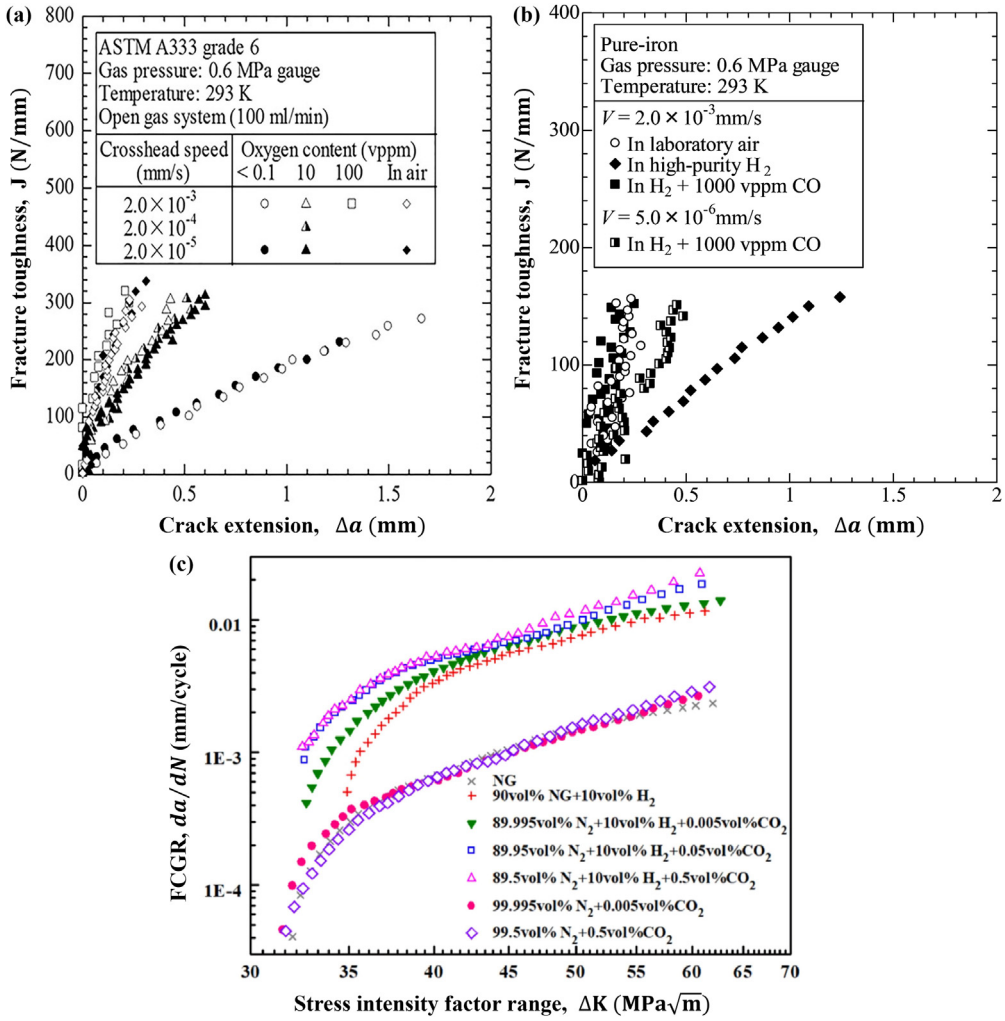

Fig. 6 – Effects of gas impurities on hydrogen embrittlement. (a): O_2 [86]; (b): CO [89]; and (c): CO_2 [90].

toughness of ASTM A333 steel at different low loading rates. Fig. 6(a) shows the fracture toughness of A333 steel returns to normal as the oxygen content increases, and the steel is barely unaffected by hydrogen when blended with the oxygen of 100-vppm. It can be concluded that blending oxygen into hydrogen effectively arrests hydrogen embrittlement. For this experiment, lower loading rates did not alter the fracture toughness of the material, thus indicating that the specimen was hydrogen saturated at these loading rates.

Similarly, Staykov et al. [89] tested the fracture toughness of pure iron in blended high-purity hydrogen with CO containing 1000-vppm. The results confirmed that the J-integral in a CO/H_2 environment was close to that obtained in the air environment, illustrating that CO could effectively inhibit hydrogen embrittlement, as shown in Fig. 6(b). However, it was found that the lower loading rates (5.0×10^{-6} mm/s) in a CO/H_2 mixture environment showed a poor inhibitory effect for hydrogen embrittlement. Moreover, Staykov et al. [89] confirmed by first-principles methods that CO does not fully adsorb to the material surface, with maximum coverage of 75% for pure iron. As a result, hydrogen atoms can still enter the material during long-term service.

Conversely, the investigation by Shang and co-workers [90] found that the adsorption of CO_2 on the surface of the specimen was significantly higher than other impurity gases in a hydrogen blending environment. The authors also demonstrated that CO_2 and H_2 collectively promoted faster FCGR as shown in Fig. 6(c). However, the mechanism of inhibition or interaction of impurity gases still requires more in-depth study for the hydrogen-blending environment.

Methods for assessment of fracture toughness

Experimental approaches. Empirical equations between the reduction in fracture toughness and hydrogen content have been developed, and they showed an exponential relationship between them [91–96]. For example, Fig. 7(a) shows the variation of CTOD for four heat treatment processes of X65 steel. These X65 steels charge in the different hydrogen charging current densities with an acid solution [97]. It can be seen that the fracture toughness, as represented by CTOD, sharply decreased at the current density between 1 mA/cm^{-2} and 2 mA/cm^{-2}, the CTOD then stabilized at 0.1 mm after the density was greater than 2 mA/cm^{-2}. The reduction in fracture toughness by hydrogen can be different for different steels.

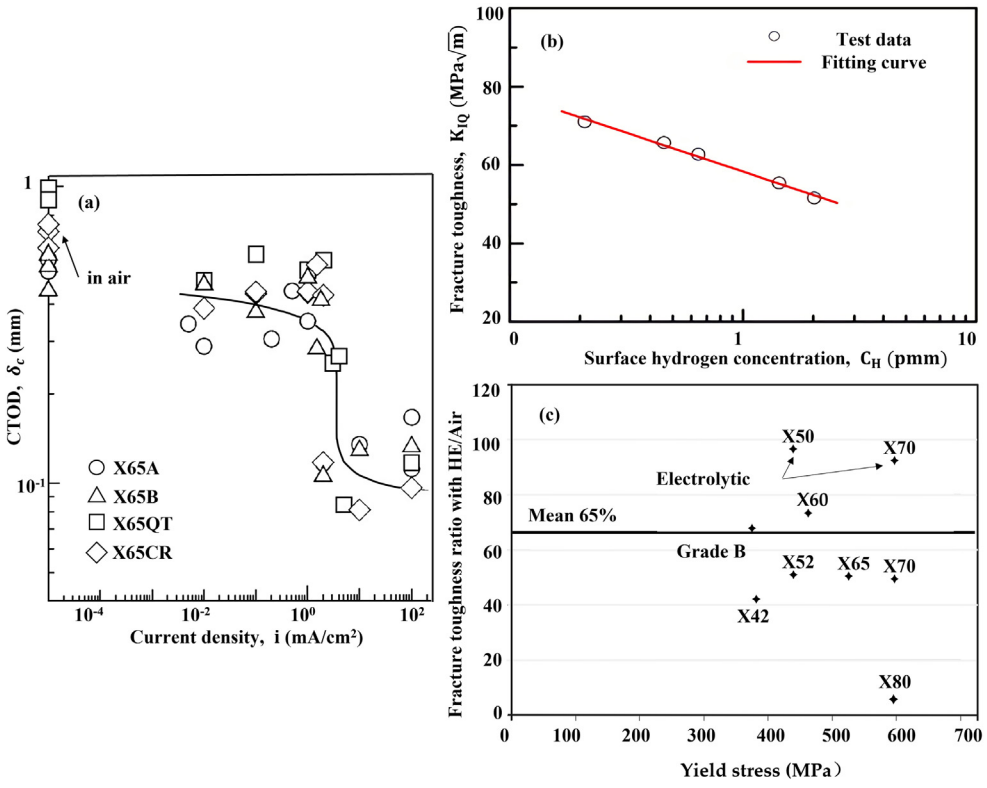

Fig. 7 – Effect of hydrogen on the fracture toughness of pipeline steel. (a) CTOD of X65 at different current densities [97]; (b) K_{IQ} of X70 at different hydrogen contents [94]; (c) Fracture toughness of different grades of pipeline steel under gaseous hydrogen [71].

Fig. 7(b) illustrates the X70 pipeline steel charged in dilute NaOH electrolyte at current densities between 10 mA/cm^{-2} and 1000 mA/cm^{-2}. Diffusible hydrogen content in the specimen is measured by the glycerol collection method. And the fracture toughness is tested at a constant displacement rate of 9.83×10^{-3} mm/min [94]. The results conclude that the hydrogen-induced fracture toughness performed a linear relationship with the logarithmic hydrogen contents, expressed as $K_{IQ} = 58.31 - 19.84\log C_H$.

A study by Pluvinage [71] found that in steels ranging from X42 to X80 steel, an average decrease of 35% in fracture toughness when exposed to 6.9 MPa gaseous hydrogen. The X80 result at a high hydrogen environment of 30.5 MPa is also shown in Fig. 7(c), showing a drastic reduction in fracture toughness when exposed to this very high-pressure hydrogen gas. Although a 30 MPa pressure is too high for the pipeline, but it is the pressure level of some of the hydrogen storage tanks installed on mobile transportations. So, the results have some application value for that type of device.

Analytical solution. The mechanism of hydrogen fracture in pipeline steel has been highly controversial due to the synergistic effects between the different mechanisms. Most researchers predict fracture toughness in hydrogen environments based on the HEDE mechanism [98–100]. Lei Fu and others [101] proposed a quantitative fracture failure criterion based on the relationship between hydrogen pressure and surface energy. A stress intensity factor (SIF) of the infinite plate model was derived considering the combined effect of hydrogen pressure and external loading. In addition, according to the HEDE mechanism, the fracture toughness of steel in hydrogen could be quantitatively predicted by Wang's model [98], as described in Eq. (4). It has also been well validated for AISI 4130, X42, and A516 steels.

$$K_{IC}^{H} \Big/ \sqrt{2\pi r} = K_{IC} \Big/ \sqrt{2\pi r} - \left(\beta S\sqrt{P} \Big/ Q\sigma_y\right) \exp\left[(2(1+\nu)V_H K_{IH} / 3RTK_{IC})Q\sigma_y\right] \quad (4)$$

where, β represents the hydrogen effect of loss in cohesive stress. V_H is partial molar volume, which is often taken as 2.0 cm^3/mol for steel. R and T are the gas constant and absolute temperature respectively. s represents the hydrogen solubility, P represents the hydrogen pressure, ν is the Poisson's ratio (for steel usually taken as 0.3), σ_y is the yield stress, Q is the work-hardening factor. However, the HELP-based model, which applies to the case of a micro void coalescence (MVC) process, has so far not been used as widely in the analytical calculations. Song et al. [102,103] are one of the few groups who recently employed the HELP model in their new hydrogen damage model to predict the fracture toughness of commercial steels based on HELP model. The error in their results was acceptable, although there remains a need for more validation at low concentrations of hydrogen.

Numerical solution. The Cohesion Zone Model (CZM) and eXtended Finite Element Methods (XFEM) can be used to simulate the crack extension behavior in a hydrogen environment [104]. In particular, the XFEM effectively avoids the

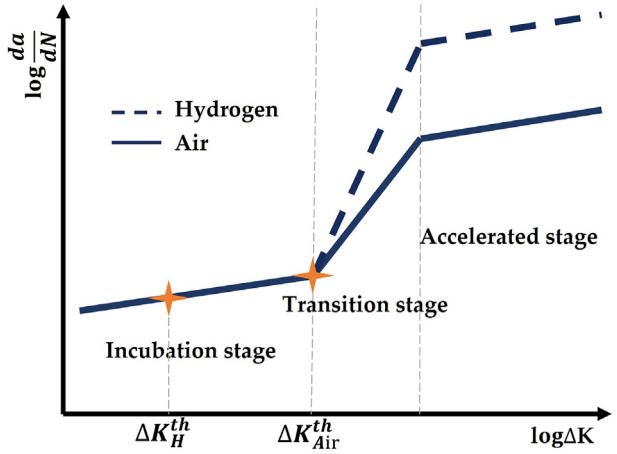

Fig. 8 – Schematic illustration of the effect of hydrogen on FCGR.

meshing discontinuities caused by the cracks introduced when setting the initial crack path. Based on the HEDE mechanism, the CZM can easily describe the damage behavior of hydrogen embrittlement in materials, which follows the Traction-Separation Law (TSL) of the interface. As the hydrogen concentration increases, the cohesive strength weakens while the accumulation increases in material damage. Therefore, developing a coupled model between the hydrogen diffusion and stress fields is key to the numerical simulations. In this model, a couple of factors should be considered, including the gradients in hydrostatic pressure and plastic strain affect hydrogen diffusion, while hydrogen diffusion accelerates material property damage.

The researchers currently redefine the ABAQUS's subroutines to couple the diffusion and stress-strain fields [105–107]. Brocks et al. [108] developed a model for explaining the mechanism of hydrogen-induced cracking, verified by the fracture experiments in ferritic steel under different displacement rates. The model illustrated that when only local softening (HELP) is considered, the material's ductility in hydrogen might be overestimated at lower loading rates. In comparison, HEDE could underestimate its ductility at higher loading rates. Thus, Brocks's model can clarify the interaction of different failure mechanisms under different loading rates.

Hydrogen effects on fatigue crack growth

Effects of hydrogen on fatigue crack growth rate

Pressure fluctuations could result in cyclic loading, which leads to fatigue damage. Fig. 8 illustrates the FCGR changes with hydrogen. The relationship between da/dN and ΔK is divided into three regions. The first region is in the crack incubation stage, where hydrogen atoms diffuse through stress-induced and accumulate at the crack tip. Hydrogen decreases the initiation threshold stress intensity factor from ΔK_{Air}^{th} to ΔK_{H}^{th}. In the second stage, the FCGR follows the Paris' law in hydrogen environment (stable FCGR phase), an increase of about one to two orders of FCGR could be observed due to hydrogen effect [109,110]. In the third region, the stress intensity factor would be increased to be close to the plane strain fracture toughness K_{IC}. In this case, FCGR can exceed the diffusible rate of hydrogen, resulting in unstable crack propagation.

Effects of loading frequency and pressure

It is widely known that decreasing frequency and increasing pressure promote FCGR. Zhang [111] observed that with increasing hydrogen pressure the size and density of the dimples on fatigue fracture surfaces gradually decrease, and more secondary cracks also appeared. Several researchers [54,112] have reported a competitive relationship between HEDE and HELP mechanisms under fatigue damage. As the local hydrogen concentration increases, HEDE phenomena play a dominant role, as evidenced by secondary cracks and intergranular cracking. Increasing the hydrogen pressure will cause the fatigue cracks to develop at a lower stress threshold. At lower frequencies, the hydrogen atoms have more time to accumulate, resulting in enrichment at the site of localized plastic deformation at the crack tip. From a macroscopic view, the cracks extend a long-distance during a given loading cycle compared with the air environment. Recent research [113] has found that, in the case of unsaturated hydrogen diffusion, the FCGR in low-carbon steel (JIS-SCM435) suddenly drops at low loading frequencies. The 'sudden drop' phenomenon has also been confirmed in pure iron (Armco iron) [114], but no researcher has verified it in pipeline steel yet. As shown in Fig. 9(a) below, the threshold frequency in this abrupt drop moves along the direction of decreasing frequency as the pressure rises and finally disappears.

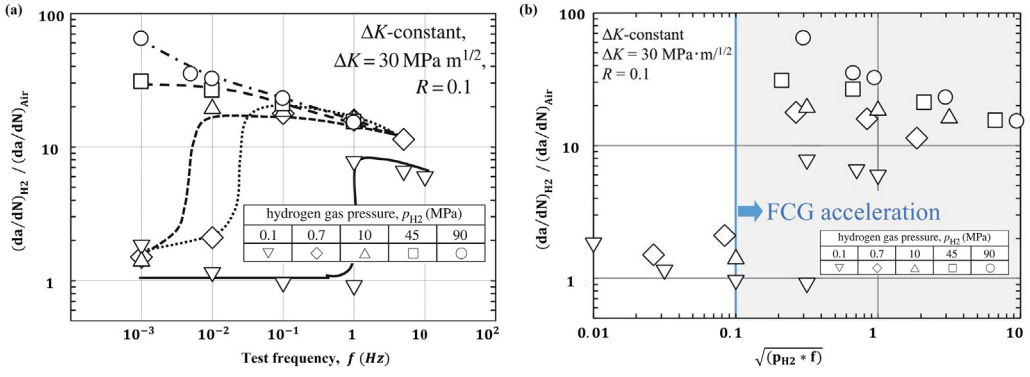

Fig. 9 – The relationship between FCGR and loading frequency at different hydrogen pressures in low-carbon steel [113].

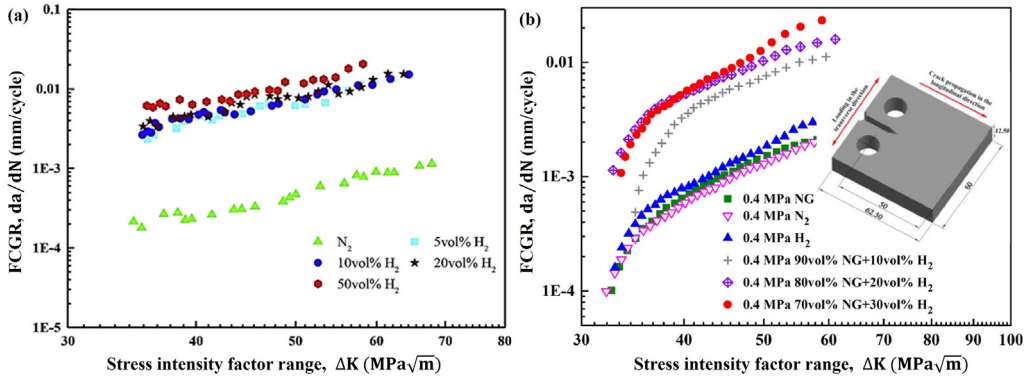

Fig. 10 – The FCGR behavior of X80 (a) and GB20# (b) steel at high or low hydrogen pressure, respectively [90,115].

Yamabe [113] believed that the acceleration in FCGR is determined by the concentration gradient of hydrogen along the crack tip. There also appears to be a critical value of localized hydrogen content that leads to an FCG acceleration. Based on Sievert's law, the concentration gradient can be calculated by the hydrogen pressure and the distance of hydrogen diffusion per unit time, as determined by the frequency. Thus, considering the coupling aspects of hydrogen pressure and frequency $(p_{H2} \times f)^{0.5}$, Fig. 9(b) shows the boundary (threshold frequency) for the sudden drop of the FCGR.

Effects of hydrogen blending ratio

Fig. 10(a) and (b) represent FCGR behavior for X80 and GB20# pipelines in high-pressure transportation systems and low-pressure distribution systems, respectively. The following figures indicated that the hydrogen-assisted FCGR of all these steels slightly changed under different hydrogen partial pressures or a natural gas-hydrogen of different concentrations, about 0.001 mm/cycle to 0.01 mm/cycle [90,115]. Furthermore, NIST and Sandia National Laboratories (SNL) [44,116] have also done extensive fatigue testing in a gaseous hydrogen environment. The FCGR results showed a negligible effect on the grades of pipeline steels.

Standards related to the design of hydrogen pipelines

Standards for design and construction of hydrogen pipelines

Regarding hydrogen pipeline design, some of the major existing codes are summarized in Table 5. The American Society of Mechanical Engineers (ASME) B31.12–2019 'Hydrogen Piping and Pipelines' and the Compressed Gas Association (CGA) G5.6-R2013 'Hydrogen Pipeline Systems' have specifications for the materials, welding and heat treatment, design, installation, and pressure testing, operation and maintenance, and non-destructive inspection of hydrogen pipelines [117]. The Chinese standard GB/T 34542 'Storage and Transportation Systems for Gaseous Hydrogen' intends to include the parts on hydrogen pipeline storage and transportation code. However, they are still in the process of being prepared.

ASME B31.12 [118] is currently the most widely recognized standard for hydrogen pipeline systems. It applies to pure or blended hydrogen piping systems with a hydrogen content greater than 10% by volume, pressures less than 21 MPa, temperatures between −62 °C and 232 °C, and a moisture content less than 20 ppm. CGA G-5.6-2013 [119] applies to the temperature range of −40 °C–175 °C; the pressure cannot exceed 21 MPa for either case.

In terms of the material selection, the ASME B31.12 document covers pipeline steels from APL 5L X42 to X80. For the grades higher than X65 steel, which are limited to maximum operating pressure (MOP) of 10.34 MPa and require compatibility testing of all materials in a hydrogen environment following Article KD-10 in ASME BPVC.VIII.3 (the Special Requirements for Vessels in Hydrogen Service of the ASME Boiler and Pressure Vessel Code, Rules for Construction of Pressure Vessels). The material parameter requirements in PSL2 include minimum impact energy, maximum tensile strength, and carbon equivalent to ensure fracture resistance and its weldability for hydrogen service. The austenitic stainless has shown good compatibility with hydrogen, but its costs are unaffordable high for long-distance applications.

Table 5 – Summary of the specifications of hydrogen transportation system.

NO.	Title	Code	Publisher
1	Hydrogen piping and pipelines	ASME B31.12–2019	ASME
2	Design guidelines for hydrogen piping and pipelines	ASME STP-PT-006-2007	ASME
3	Hydrogen Pipeline System	CGA G5.6-R2013	CGA
4	Hydrogen Pipeline System	AIGA 033-2014	AIGA
5	Storage and Transportation Systems for Gaseous Hydrogen—Part 5: the specification of gaseous hydrogen transportation system[a]	GB/T 34542.5	SAC

AIGA: Asia Industrial Gases Association; SAC: Standardization Administration of the P.R.C.; GB/T: Chinese Standard.
[a] This document is still in the preparation.

Both standards require higher fracture toughness of pipeline steels for a hydrogen environment than for other energy media and this is done by controlling metallurgical factors. ASME B31.12 limits the alloying elements in terms of carbon content (0.07%), sulfur content (0.007%), phosphorus content (0.015%), carbon equivalent Pcm (0.15% for X52 to X60, and 0.17% for X65 to X80) for high-strength micro-alloy steel (HSLA) when the hoop stress exceeds its SMYS of 40%. While the CGA G5.6 limits micro-alloyed steels with sulfur (0.01%), phosphorus (0.015%), and carbon equivalent CEs (0.35%).

ASME B31.12 requires pipe steels to have a microstructure of polygonal and needle-like ferrite that is uniformly distributed in the cross-section. It recommends a grain size less than ASTM 9 and banding in the structure of no more than 1.5 grades for a high-pressure hydrogen environment. However, CGA only requires the grain size no larger than ASTM Grade 8. In terms of the hardness of the weld area, ASME B31.12 and CGA provide the hardness requirements in the welding region, which are 235 HV10 and 22 HRC (equal to 250 HV10), respectively. Overall, the ASME B31.12 document shows the higher and more strict requirements for materials in hydrogen gas service.

In regard to thickness requirements in pipeline design, by ASME B31.12 the wall thickness t at design pressure P could be determined by Eq. (5). It considers an additional factor of material performance H_f compared with ASME B31.8, which is for oil and gas pipeline design code. The coefficient H_f decreases with increasing yield strength and design pressure. Therefore, the method described by Eq. (5) is to guard against hydrogen embrittlement by increasing the wall thickness.

$$t = PD/2SFETH_f \tag{5}$$

where, t is the nominal wall thickness, P is the design pressure, D is the outer diameter of the pipe, S is the minimum yield stress, F and T are the strength design factor and temperature derating factor, respectively. T obtained from the Table PL-3.7.1 in ASME B31.12 document, usually taken as 1.0 when test temperature below 120 °C. E is the weld factor, taken as 1.0 for pipeline steel generally. H_f is the material performance factor.

In addition, ASME B31.12 also offers two methods for controlling the fracture of pipelines when the hoop stress exceeds 40% of SMYS. One of these is the prescriptive design method of pipeline, named Option A in the following description. To arrest brittle fracture, the shear area of the Charpy and drop-weight tear testing specimens (0 °C or lower) should be seen in more than 80% and 40% of their fracture surface, respectively. And the Charpy energy values of the pipe must be greater than that calculated using Eq. (6) below, for ensuring adequate resistance. CGA G-5.6 simply specifies the impact energy (0 °C) greater than 94 J(T) and 118 J.

$$CVN = 0.008(rt)^{0.39}\sigma_h^2 \tag{6}$$

where CVN is the full-size specimen energy (0 °C), r is the pipe radius, t is the pipe wall thickness, σ_h is the hoop stress.

Option A is mainly based on the conservative design parameters to increase the safety of the hydrogen pipeline. This includes a material performance factor H_f as mentioned before, and a design factor F, where the values for the design factor F is reduced to 0.5 in the Class I Area (compared to 0.72 for natural gas pipelines).

Another option, Option B, is based on the material performance design method. The value of F for this approach remains unchanged compared with the oil and gas pipeline design code. And the thickness factor H_f is usually taken as 1.0. However, Option B requires designed materials to be tested in a hydrogen environment. The test procedure should follow Article KD-10. And it also limits the threshold stress intensity factor K_{th} to be equal or greater than the applied stress intensity factors K_{IA}, which calculated by the critical size of an elliptical surface crack at the design pressure, and also K_{IH} should be higher than 54 MPa$\sqrt{m}$.

Determination of K_{IH} and K_{IC}

The threshold stress intensity factor K_{IH} and plane-strain fracture toughness K_{IC} can be tested by the rising-load method, where the specimen is loaded at a constant displacement rate. The test procedure follows the ASTM E1820 code 'Test Method for Measurement of Fracture Toughness'. The initial threshold stress intensity is determined by the deviation point in the load-displacement curve, which can be approximated as the endpoint when the load rises linearly, or by recording the critical load of crack initiation using acoustic emission techniques. In order to obtain conservative evaluation results, the evaluation of mechanical parameters such as K_{IH} and K_{IC} in a hydrogen environment requires that the strain rate at the crack tip is low enough to ensure that the local hydrogen concentration at the crack tip is saturated [120].

The loading rate of the plane-strain fracture toughness test is not mentioned in Article KD-10, but in the ANSI/CSA CHMC-1 and GB/T 34542.2, both recommend that the rate of stress intensity factor should be between 0.1 MPa$\sqrt{m}$ to 1 MPa$\sqrt{m}$/minat the linear elastic stage. As illustrated in the following analysis, this 0.1 MPa$\sqrt{m}$/min may still be too fast for the real service conditions.

Slow geological movement sometime experienced by pipelines can result in axial stresses in the vulnerable

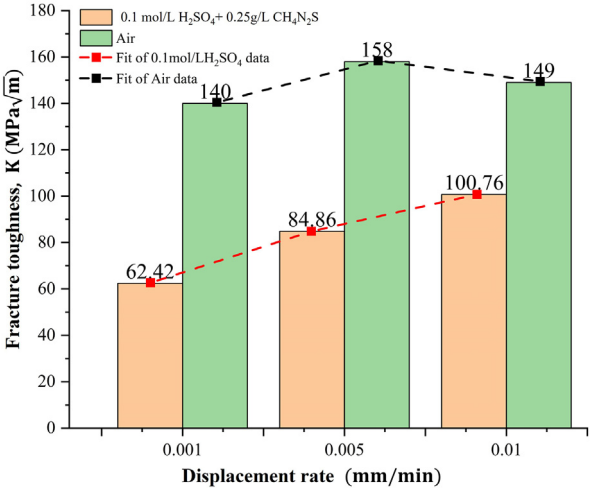

Fig. 11 – The fracture toughness of GB20# steel at different displacement rates.

segments of a pipeline route. Such loading due to ground activity usually occurs at a slow rate. For this reason, we studied the fracture toughness of GB20# steel at a slow displacement rate, and the three-point bending specimens of such steel were H charged using acidic solution inhibited by thiourea. The results showed that the fracture toughness was highly sensitive to the loading rate, whereas the fracture toughness in an air environment is independent of the loading rate, as shown in Fig. 11.

When the slow displacement rate is applied, a sufficient amount of time is allowed for hydrogen to diffuse to the crack initiation site, and in particular, to accumulate in the region of high stress and high strain. Therefore, a slow loading rate gives the crack tip region an opportunity to become more hydrogen enriched, resulting in the decrease of fracture toughness.

In the current standard, the recommended rate of loading is quite fast for slow axial-loading conditions, as mentioned before. It is well possible that the fracture toughness of a steel (a GB20# steel as in the case of our study) has not reached its plateau when tests were done at the crosshead displacement rate of 0.001 mm/min (it equals to an increase at average rate of 0.011 MPa$\sqrt{m}$/min for the SIF rises), and it is well possible that lower displacement rates could result in even lower fracture toughness value. Therefore, we suggest even slower loading rates be used, in terms of the rate of SIF, in order to cover such slow loading conditions in the real service.

As an example, we consider a part-through crack in a 305 mm diameter pipe. The SIF at the crack tip can be estimated by combining the contributions of the internal pressure and the axial load to the SIF [121,122]. The SIF for a axially oriented crack, with a depth of 50% of wall thickness of 4.8 mm, under a pressure of 6 MPa can be calculated to be approximately 48 MPa$\sqrt{m}$[123]. When the SIF increase, under slow axial loading, from 48 MPa$\sqrt{m}$ to its fracture toughness, say, about 150 MPa$\sqrt{m}$, the rate of SIF increase can be calculated about 0.071 MPa$\sqrt{m}$/min if the axial loading occurs in a day, or about 0.010 MPa$\sqrt{m}$/min if the axial loading occurs in a week. All these estimated rates are much lower than the rates in the CSA standard. Therefore, it is evident that the current test standard can give non-conservative toughness results and there is a need to perform toughness testing of H charged samples at lower loading rates.

Challenges and opportunities

- Material selection: The pipeline steels that have been used for delivering hydrogen were usually made of materials of low grade, no higher than X52. To improve efficiency, higher-grade pipelines need to be built to transport high-pressure hydrogen. However, poor fracture toughness is the main concern for high-grade pipelines for hydrogen transportation, as stated in some literature [124].
  Extensive literature [12,84,92,124,125] proved that the higher-grade pipeline steels show high HE susceptibility. From a microscopic view, the HE sensitivity of microstructure follows an increasing order of acicular ferrite, polygonal ferrite, and bainite. For the present, the microstructure of polygonal ferrite/acicular ferrite in commercial API pipeline steels performed better fracture toughness at a higher pressure of hydrogen, up to 21 MPa [126]. Therefore, researchers ought to consider redesigning the microstructure of existing high-grade pipeline steel for enhanced resistance of HE.

- Welding: Optimizing the weld hydrogen resistance in the girth welds is an unavoidable challenge for hydrogen pipelines. The present research on improving the hydrogen resistance of the girth welds and their welding techniques is still inadequate, in particular, in controlling the residual stress on the girth welds[[127]. From the above discussion, it can be concluded that selecting suitable hydrogen-resistant welding consumables and controlling the heat input and the cooling rate for preventing the generation of inclusions, M/A constituents and other hard phases. These are effective ways to improve the hydrogen resistance in the weld region.
- Demo projects of hydrogen pipelines at high pressures: One of the current challenges is the lack of demonstrations of high-strength pipelines used in high-pressure hydrogen transport. In addition, another is the lack of demonstrations of hydrogen blending for existing metallic pipelines. Existing natural gas pipelines may already suffer from stress corrosion and mechanical damage, and poor-quality girth welds can accelerate the hydrogen embrittlement effects. At the same time, loading conditions such as internal pressure fluctuations or geological movement also exacerbate the failure.

Concluding remarks

This paper reviews the key features of international and domestic demonstration projects for hydrogen transportation by pipeline, including their specifications and operating parameters. In addition, the factors affecting the hydrogen compatibility with pipeline steel is described in terms of the steel microstructure, mechanical parameters, and environmental factors. The ductility and fracture properties of pipeline steel under slow loading are significantly reduced, while the crack growth rate under fatigue loading is dramatically increased by the presence of hydrogen, sometimes by one to two orders of magnitude. The following conclusions can be drawn:

- Some of the hydrogen natural gas blending projects showed that PE pipes are compatible with hydrogen, and they can be used for low-pressure hydrogen distribution. The hydrogen transport demonstration projects with hydrogen pressure between 3 and 5 MPa proved that high-ductility low carbon steels, such as API 5L Grade B/X42/X52, can be used.
- Although the ASME B31.12 and CGA G5.6 standards both allow pipeline pressure up to 21 MPa, in reality, there are few projects of hydrogen pipelines with pressure greater than 10 MPa at this time.

- Various welding studies and related failure analyses showed that the girth welds are prone to hydrogen damage as they are susceptible to have inhomogeneous distribution in microstructure and uneven hardness, high residual tensile stresses, and small defects generated during welding, which can cause localized hydrogen accumulation. Improving the hydrogen resistance of welds remains an important issue for future research.
- On the basis of mechanistic studies surveyed in this study, it is clear that the interaction between diffusible hydrogen and dislocation pre-dominant aspects in the hydrogen embrittlement process causing deterioration of the mechanical properties of pipelines, and only when the local hydrogen concentration reaches its critical value (c_{th}), does the hydrogen embrittlement occurs under tensile loading. The coupling of these factors means the occurrence of cracking is affected by both the hydrogen concentrations and loading conditions. If the loading rate or frequency is too fast, it will not be sufficient for hydrogen diffuse to the susceptible sites to produce an embrittlement effect. Therefore, in the compatibility assessment either fracture toughness or fatigue test the selection of the loading rate or frequency is essential. For example, the transition of low fatigue crack growth rate to fast growth rate can happen at different frequencies for different hydrogen levels involved.
- The axial load caused by geological movement and ground settlement can be quite slow for buried pipelines. The author's own work showed that when the loading rate was lowered from a dK/dt value of 0.1 to 0.01 MPa$\sqrt{m}$/min the toughness parameter K_{IC} continued to decrease with the loading rate when hydrogen is contained in the test steels. The current test standard, which specifies range of loading rate between 0.1 and 1 MPa$\sqrt{m}$/min, can give non-conservative toughness results. Therefore, the test conditions and test codes for compatibility testing should be modified to cover the slow-loading cases that may arise in actual operating conditions.
- The papers reviewed indicate that the addition of gases such as O_2 and CO can have a significant effect in inhibiting hydrogen embrittlement. This is an interesting finding; if it is proven to be a universal effect for different grades of steel, it may well provide an interesting mitigation solution for the high-pressure hydrogen pipelines.

Declaration of competing interest

The authors declare that they have no known competing financial interests or personal relationships that could have appeared to influence the work reported in this paper.

Acknowledgment

This work was supported by the Key Area Research and Development Program of Guangdong Province, China (Number: 2019B111102001), and the Beijing Municipal Science and Technology Commission, China (Number: Z201100004520011).

REFERENCES

[1] Shu G, Zhang H, Mi W. Reinventing the economy and reversing the path to global warming climate change: an analysis of the dynamics of the hydrogen economy. China: Shanghai University; 2021.
[2] Gondal IA. Hydrogen integration in power-to-gas networks. Int J Hydrogen Energy 2019;44:1803–15. https://doi.org/10.1016/J.IJHYDENE.2018.11.164.
[3] Obara S, Li J. Evaluation of the introduction of a hydrogen supply chain using a conventional gas pipeline–A case study of the Qinghai–Shanghai hydrogen supply chain. Int J Hydrogen Energy 2020;45:33846–59. https://doi.org/10.1016/j.ijhydene.2020.09.009.
[4] Miao B, Giordano L, Chan SH. Long-distance renewable hydrogen transmission via cables and pipelines. Int J Hydrogen Energy 2021;46:18699–718. https://doi.org/10.1016/j.ijhydene.2021.03.067.
[5] Wu W-P, Wu K-X, Zeng W-K, Yang P-C. Optimization of long-distance and large-scale transmission of renewable hydrogen in China: pipelines vs. UHV. Int J Hydrogen Energy 2022;47:24635–50. https://doi.org/10.1016/j.ijhydene.2021.10.066.
[6] Liu B, Liu S, Guo S, Zhang S. Economic study of a large-scale renewable hydrogen application utilizing surplus renewable energy and natural gas pipeline transportation in China. Int J Hydrogen Energy 2020;45:1385–98. https://doi.org/10.1016/j.ijhydene.2019.11.056.
[7] Nazir H, Muthuswamy N, Louis C, Jose S, Prakash J, Buan ME, et al. Is the H2 economy realizable in the foreseeable future? Part II: H2 storage, transportation, and distribution. Int J Hydrogen Energy 2020;45:20693–708. https://doi.org/10.1016/j.ijhydene.2020.05.241.
[8] Faye O, Szpunar J, Eduok U. A critical review on the current technologies for the generation, storage, and transportation of hydrogen. Int J Hydrogen Energy 2022;47:13771–802. https://doi.org/10.1016/j.ijhydene.2022.02.112.
[9] IEA. The Future of hydrogen, Seizing today's opportunities. Int Energy Agency; 2019. https://www.iea.org/reports/the-future-of-hydrogen. [Accessed 25 April 2022].
[10] Haeseldonckx D, D'haeseleer W. The use of the natural-gas pipeline infrastructure for hydrogen transport in a changing market structure. Int J Hydrogen Energy 2007;32:1381–6. https://doi.org/10.1016/j.ijhydene.2006.10.018.
[11] Castello P, Tzimas E, Moretto P, Peteves SD. Techno-economic assessment of hydrogen transmission and distribution systems in Europe in the medium and long term. https://www.osti.gov/etdeweb/biblio/21011978. [Accessed 25 April 2022].
[12] Dwivedi SK, Vishwakarma M. Hydrogen embrittlement in different materials: a review. Int J Hydrogen Energy 2018;43:21603–16. https://doi.org/10.1016/J.IJHYDENE.2018.09.201.
[13] Ohaeri E, Eduok U, Szpunar J. Hydrogen related degradation in pipeline steel: a review. Int J Hydrogen Energy 2018;43:14584–617. https://doi.org/10.1016/J.IJHYDENE.2018.06.064.
[14] Sun Y, Frank Cheng Y. Hydrogen-induced degradation of high-strength steel pipeline welds: a critical review. Eng Fail Anal 2022;133:105985. https://doi.org/10.1016/J.ENGFAILANAL.2021.105985.
[15] Wu X, Zhang H, Yang M, Jia W, Qiu Y, Lan L. From the perspective of new technology of blending hydrogen into natural gas pipelines transmission: mechanism, experimental study, and suggestions for further work of hydrogen embrittlement in high-strength pipeline steels.

Int J Hydrogen Energy 2022;47:8071–90. https://doi.org/10.1016/J.IJHYDENE.2021.12.108.
[16] Mohitpour M, Solanky H, Vinjamuri GK. Materials selection and performance criteria for hydrogen pipeline transmission. Am. Soc. Mech. Eng. Press. Vessel. Pip. Div. PVP, vol. 475. ASMEDC; 2004. p. 241–51. https://doi.org/10.1115/PVP2004-2564.
[17] Strategy&. HyWay 27: realisation of a national hydrogen network. https://www.hyway27.nl/en/latest-news/hyway-27-realisation-of-a-national-hydrogen-network. [Accessed 12 March 2022].
[18] Air Products hydrogen pipeline project. https://ceqanet.opr.ca.gov/2020059038/4. [Accessed 11 March 2022].
[19] Fekete JR, Sowards JW, Amaro RL. Economic impact of applying high strength steels in hydrogen gas pipelines. Int J Hydrogen Energy 2015;40:10547–58. https://doi.org/10.1016/j.ijhydene.2015.06.090.
[20] U.S.Department of Energy. Final report - hydrogen delivery infrastructure options analysis. https://www.energy.gov/eere/fuelcells/downloads/final-report-hydrogen-delivery-infrastructure-options-analysis. [Accessed 25 April 2022].
[21] Melaina MW, Antonia O, Penev M. Blending hydrogen into natural gas pipeline networks. Golden, CO (United States). https://doi.org/10.2172/1068610; 2013.
[22] Tiekstra GC, Koopman FP. The NATURALHY project: first step in assessing the potential of the existing natural gas network for hydrogen delivery. Int. Gas Res. Conf. Proc. 2008;2:1509–18.
[23] Gahleitner G. Hydrogen from renewable electricity: an international review of power-to-gas pilot plants for stationary applications. Int J Hydrogen Energy 2013;38:2039–61. https://doi.org/10.1016/J.IJHYDENE.2012.12.010.
[24] Kippers MJ, De Laat JC, Hermkens RJM, Overdiep JJ, Van Der Molen A, Van Erp WC, et al. Pilot project on hydrogen injection in natural gas on Island of Ameland in The Netherlands. Int. Gas Union Res. Conf. 2011:19–21.
[25] Mainz Energie Park. Project aims. https://www.energiepark-mainz.de/en/project/project-aims/. [Accessed 12 March 2022].
[26] HyDeploy Isaac T. The UK's first hydrogen blending deployment project. Clean Energy 2019;3:114–25. https://doi.org/10.1093/CE/ZKZ006.
[27] Snam. Hydrogen blend doubled to 10% in Contursi trial. https://www.snam.it/en/Media/news_events/2020/Snam_hydrogen_blend_doubled_in_Contursi_trial.html. [Accessed 30 July 2021].
[28] HyBlend project to accelerate potential for blending hydrogen in natural gas pipelines | news | NREL. https://www.nrel.gov/news/program/2020/hyblend-project-to-accelerate-potential-for-blending-hydrogen-in-natural-gas-pipelines.html. [Accessed 29 July 2021].
[29] H-Mat. https://h-mat.org/. [Accessed 8 December 2021].
[30] Falkenhagen WindGas. Pioneering green gas production. https://www.powermag.com/windgas-falkenhagen-pioneering-green-gas-production/. [Accessed 30 July 2021].
[31] Communication D de la, (France) GRDF-G, (France) S des transports de D et extensions-S, Ineo E, (France) Gnv-E, (France) AH. Grhyd - management of Networks by injection of Hydrogen to De-carbonate energies. Press file. The GRHYD project partners inaugurate the first Power-to-Gas demonstrator in France. et al.. 2018.
[32] Hartley PG, Au V. Towards a large-scale hydrogen industry for Australia. Engineering 2020;6:1346–8. https://doi.org/10.1016/j.eng.2020.05.024.
[33] Klopffer M-H, Berne P, Espuche É. Development of innovating materials for distributing mixtures of hydrogen and natural gas. Study of the barrier properties and durability of polymer pipes. Oil Gas Sci Technol – Rev d'IFP Energies Nouv 2015;70:305–15. https://doi.org/10.2516/ogst/2014008.
[34] Haines M, Polman E, Delaat J. Reduction of CO2 emissions by addition of hydrogen to natural gas. Greenh. Gas Control Technol. 7. Proceedings of the 7th International Conference on Greenhouse Gas Control Technologies 2005;5:337–45. https://doi.org/10.1016/B978-008044704-9/50035-5.
[35] Dodds PE, Demoullin S. Conversion of the UK gas system to transport hydrogen. Int J Hydrogen Energy 2013;38:7189–200. https://doi.org/10.1016/j.ijhydene.2013.03.070.
[36] Us DRIVE. Fuel cell technical team roadmap. USA: United States Driving Research and Innovation for Vehicle efficiency and Energy sustainability; 2017.
[37] Zhanfeng G. Cause analysis of welding crack with hydrogen pipeline. HEBEI Chem Ind 2013;36:61–4.
[38] Zhou G, Tong Z, Chen X, Zheng W, Xiong D, Wang Y. A review on the welding of X80 pipeline steel and factors affecting weld cracking. Mater Reports 2022;36. https://doi.org/10.11896/CLDB.21100169. 21100169–9.
[39] Djukic MB, Bakic GM, Sijacki Zeravcic V, Sedmak A, Rajicic B. The synergistic action and interplay of hydrogen embrittlement mechanisms in steels and iron: localized plasticity and decohesion. Eng Fract Mech 2019;216:106528. https://doi.org/10.1016/J.ENGFRACMECH.2019.106528.
[40] Dear FF, G Skinner GC, Kirchheim R, Yue S. Mechanisms of hydrogen embrittlement in steels: discussion. Philos Trans R Soc A Math Phys Eng Sci 2017;375. https://doi.org/10.1098/RSTA.2017.0032.
[41] Xing X, Zhang H, Cui G, Liu J, Li Z. Hydrogen inhibited phase transition near crack tip – an atomistic mechanism of hydrogen embrittlement. Int J Hydrogen Energy 2019;44:17146–53. https://doi.org/10.1016/J.IJHYDENE.2019.04.205.
[42] Song J, Curtin WA. Atomic mechanism and prediction of hydrogen embrittlement in iron. Nat Mater 2013;12:145–51. https://doi.org/10.1038/nmat3479.
[43] Ogawa Y, Matsunaga H, Yamabe J, Yoshikawa M, Matsuoka S. Unified evaluation of hydrogen-induced crack growth in fatigue tests and fracture toughness tests of a carbon steel. Int J Fatigue 2017;103:223–33. https://doi.org/10.1016/j.ijfatigue.2017.06.006.
[44] Slifka AJ, Drexler ES, Amaro RL, Hayden LE, Stalheim DG, Lauria DS, et al. Fatigue measurement of pipeline steels for the application of transporting gaseous hydrogen. J Pressure Vessel Technol 2018;140. https://doi.org/10.1115/1.4038594.
[45] Park C, Kang N, Liu S. Effect of grain size on the resistance to hydrogen embrittlement of API 2W Grade 60 steels using in situ slow-strain-rate testing. Corrosion Sci 2017;128:33–41. https://doi.org/10.1016/J.CORSCI.2017.08.032.
[46] Trögerq M, Boschq C, Wiartw J-N, Meusere H, Knoopr FM, Brauert H, et al. Investigations on hydrogen assisted cracking of welded high-strength pipes in gaseous hydrogen. Steely Hydrog. Conf. 2014;10&11&12.
[47] Mostafijur Rahman KM, Mohtadi-Bonab MA, Ouellet R, Szpunar J, Zhu N. Effect of electrochemical hydrogen charging on an API X70 pipeline steel with focus on characterization of inclusions. Int J Press Vessel Pip 2019;173:147–55. https://doi.org/10.1016/j.ijpvp.2019.05.006.
[48] Xue HB, Cheng YF. Characterization of inclusions of X80 pipeline steel and its correlation with hydrogen-induced cracking. Corrosion Sci 2011;53:1201–8. https://doi.org/10.1016/j.corsci.2010.12.011.
[49] Lam PS, Sindelar RL, Duncan AJ, Adams TM. Literature survey of gaseous hydrogen effects on the mechanical properties of carbon and low alloy steels, vol. 131. J Press Vessel Technol Trans ASME; 2009. https://doi.org/10.1115/1.3141435.

[50] Ayas C, Deshpande VS, Fleck NA. A fracture criterion for the notch strength of high strength steels in the presence of hydrogen. J Mech Phys Solids 2014;63:80–93. https://doi.org/10.1016/J.JMPS.2013.10.002.
[51] Novak P, Yuan R, Somerday BP, Sofronis P, Ritchie RO. A statistical, physical-based, micro-mechanical model of hydrogen-induced intergranular fracture in steel. J Mech Phys Solids 2010;58:206–26. https://doi.org/10.1016/J.JMPS.2009.10.005.
[52] Peng Z, Liu J, Huang F, Hu Q, Cao C, Hou S. Comparative study of non-metallic inclusions on the critical size for HIC initiation and its influence on hydrogen trapping. Int J Hydrogen Energy 2020;45:12616–28. https://doi.org/10.1016/J.IJHYDENE.2020.02.131.
[53] Chatzidouros EV, Papazoglou VJ, Tsiourva TE, Pantelis DI. Hydrogen effect on fracture toughness of pipeline steel welds, with in situ hydrogen charging. Int J Hydrogen Energy 2011;36:12626–43. https://doi.org/10.1016/j.ijhydene.2011.06.140.
[54] Gao Z, Gong B, Wang B, Wang D, Deng C, Yu Y. Effect of fatigue damage on the hydrogen embrittlement sensitivity of X80 steel welded joints. Int J Hydrogen Energy 2021;46:38535–50. https://doi.org/10.1016/J.IJHYDENE.2021.09.090.
[55] Ronevich JA, Song EJ, Somerday BP, San Marchi CW. Hydrogen-assisted fracture resistance of pipeline welds in gaseous hydrogen. Int J Hydrogen Energy 2021;46:7601–14. https://doi.org/10.1016/J.IJHYDENE.2020.11.239.
[56] Ronevich J, Kolasinski R, Bartelt N, Somerday B, Marchi CS, Thurmer K, et al. Oxygen impurity effects on hydrogen assisted fatigue and fracture of X100 pipeline steel. Am Soc Mech Eng Press Vessel Pip Div PVP; 2018. https://doi.org/10.1115/PVP2018-84163. 6B-2018.
[57] Sun Y, Cheng YF. Hydrogen permeation and distribution at a high-strength X80 steel weld under stressing conditions and the implication on pipeline failure. Int J Hydrogen Energy 2021;46:23100–12. https://doi.org/10.1016/J.IJHYDENE.2021.04.115.
[58] Zhang T, Wang Y, Zhao W, Tang X, Du T, Yang M, et al. Hydrogen permeation parameters of X80 steel and welding HAZ under high pressure coal gas environment. Acta Met Sin 2015;51:1101–10. https://doi.org/10.11900/0412.1961.2015.00039.
[59] Turnbull A, Koers RWJ, Gutiérrez-Solana F, Álvarez JA. Environment induced cracking: a fitness for service perspective. In: 24th int. Conf. Offshore mech. Arct. Eng., vol. 3. ASMEDC; 2005. p. 339–43. https://doi.org/10.1115/OMAE2005-67566.
[60] Xu K, ying Qiao G, yan Pan X, wei Chen X, Liao B, ren Xiao F. Simulation of fatigue properties for the weld joint of the X80 weld pipe before and after removing the weld reinforcement. Int J Press Vessel Pip 2020;187:104164. https://doi.org/10.1016/J.IJPVP.2020.104164.
[61] Yokobori AT, Chinda Y, Nemoto T, Satoh K, Yamada T. The characteristics of hydrogen diffusion and concentration around a crack tip concerned with hydrogen embrittlement. Corrosion Sci 2002;44:407–24. https://doi.org/10.1016/S0010-938X(01)00095-6.
[62] Takakuwa O, Nishikawa M, Soyama H. Numerical simulation of the effects of residual stress on the concentration of hydrogen around a crack tip. Surf Coatings Technol 2012;206:2892–8. https://doi.org/10.1016/J.SURFCOAT.2011.12.018.
[63] Zhao W, Yang M, Zhang T, Deng Q, Jiang W, Jiang W. Study on hydrogen enrichment in X80 steel spiral welded pipe. Corrosion Sci 2018;133:251–60. https://doi.org/10.1016/J.CORSCI.2018.01.011.
[64] Mirzaee-Sisan A, Wu G. Residual stress in pipeline girth welds- A review of recent data and modelling. Int J Press Vessel Pip 2019;169:142–52. https://doi.org/10.1016/J.IJPVP.2018.12.004.
[65] Ronevich JA, D'Elia CR, Hill MR. Fatigue crack growth rates of X100 steel welds in high pressure hydrogen gas considering residual stress effects. Eng Fract Mech 2018;194:42–51. https://doi.org/10.1016/J.ENGFRACMECH.2018.02.030.
[66] Nanninga NE, Levy YS, Drexler ES, Condon RT, Stevenson AE, Slifka AJ. Comparison of hydrogen embrittlement in three pipeline steels in high pressure gaseous hydrogen environments. Corrosion Sci 2012;59:1–9. https://doi.org/10.1016/j.corsci.2012.01.028.
[67] Park C, Kang N, Liu S. Effect of grain size on the resistance to hydrogen embrittlement of API 2W Grade 60 steels using in situ slow-strain-rate testing. Corrosion Sci 2017;128:33–41. https://doi.org/10.1016/j.corsci.2017.08.032.
[68] Duncan A, Lam P-S, Adams T. Tensile testing of carbon steel in high pressure hydrogen, 6 Mater. ASMEDC: Fabr.; 2007. p. 519–25. https://doi.org/10.1115/PVP2007-26736.
[69] Brass AM, Chêne J. Influence of tensile straining on the permeation of hydrogen in low alloy Cr-Mo steels. Corrosion Sci 2006;48:481–97. https://doi.org/10.1016/j.corsci.2005.01.007.
[70] Zhou D, Li T, Huang D, Wu Y, Huang Z, Xiao W, et al. The experiment study to assess the impact of hydrogen blended natural gas on the tensile properties and damage mechanism of X80 pipeline steel. Int J Hydrogen Energy 2021;46:7402–14. https://doi.org/10.1016/j.ijhydene.2020.11.267.
[71] Pluvinage G. Mechanical properties of a wide range of pipe steels under influence of pure hydrogen or hydrogen blended with natural gas. Int J Press Vessel Pip 2021;190:104293. https://doi.org/10.1016/J.IJPVP.2020.104293.
[72] Nguyen TT, Park J, Kim WS, Nahm SH, Beak UB. Effect of low partial hydrogen in a mixture with methane on the mechanical properties of X70 pipeline steel. Int J Hydrogen Energy 2020;45:2368–81. https://doi.org/10.1016/J.IJHYDENE.2019.11.013.
[73] Zheng Y, Zhang L, Shi Q, Zhou C, Zheng J. Effects of hydrogen on the mechanical response of X80 pipeline steel subject to high strain rate tensile tests. Fatig Fract Eng Mater Struct 2020;43:684–97. https://doi.org/10.1111/FFE.13151.
[74] Fukunaga A. Differences between internal and external hydrogen effects on slow strain rate tensile test of iron-based superalloy A286. Int J Hydrogen Energy 2022;47:2723–34. https://doi.org/10.1016/J.IJHYDENE.2021.10.178.
[75] Ferreira PJ, Robertson IM, Birnbaum HK. Hydrogen effects on the interaction between dislocations. Acta Mater 1998;46:1749–57. https://doi.org/10.1016/S1359-6454(97)00349-2.
[76] Han YD, Wang RZ, Wang H, Xu LY. Hydrogen embrittlement sensitivity of X100 pipeline steel under different pre-strain. Int J Hydrogen Energy 2019;44:22380–93. https://doi.org/10.1016/J.IJHYDENE.2019.06.054.
[77] Maier HJ, Popp W, Kaesche H. Effects of hydrogen on ductile fracture of a spheroidized low alloy steel. Mater Sci Eng, A 1995;191:17–26. https://doi.org/10.1016/0921-5093(94)09623-5.
[78] Tien J, Thompson AW, Bernstein IM, Richards RJ. Hydrogen transport by dislocations. Metall Trans A 1976;7:821–9. https://doi.org/10.1007/BF02644079. 76 1976.
[79] Zhou C, Ye B, Song Y, Cui T, Xu P, Zhang L. Effects of internal hydrogen and surface-absorbed hydrogen on the hydrogen embrittlement of X80 pipeline steel. Int J

Hydrogen Energy 2019;44:22547–58. https://doi.org/10.1016/j.ijhydene.2019.04.239.
[80] Birnbaum HK, Sofronis P. Hydrogen-enhanced localized plasticity—a mechanism for hydrogen-related fracture. Mater Sci Eng, A 1994;176:191–202. https://doi.org/10.1016/0921-5093(94)90975-X.
[81] Onyewuenyi OA, Hirth JP. Effects of hydrogen on notch ductility and fracture in spheroidized AISI 1090 steel. Metall Trans A 1983;14:259–69. https://doi.org/10.1007/BF02651623. 141 1983.
[82] Bieganski Z, Ableiter M, Gonser U, Oriani RA. A mechanistic theory of hydrogen embrittlement of steels. Berichte Der Bunsengesellschaft Für Phys Chemie 1972;76:848–57. https://doi.org/10.1002/BBPC.19720760864.
[83] Song EJ, Bhadeshia HKDH, Suh DW. Effect of hydrogen on the surface energy of ferrite and austenite. Corrosion Sci 2013;77:379–84. https://doi.org/10.1016/J.CORSCI.2013.07.043.
[84] Capelle J, Gilgert J, Dmytrakh I, Pluvinage G. The effect of hydrogen concentration on fracture of pipeline steels in presence of a notch. Eng Fract Mech 2011;78:364–73. https://doi.org/10.1016/J.ENGFRACMECH.2010.10.007.
[85] Nibur KA, Somerday BP. Fracture and fatigue test methods in hydrogen gas. USA: Woodhead Publishing; 2012. https://doi.org/10.1533/9780857093899.2.195.
[86] Komoda R, Kubota M, Staykov A, Ginet P, Barbier F, Furtado J. Inhibitory effect of oxygen on hydrogen-induced fracture of A333 pipe steel. Fatig Fract Eng Mater Struct 2019;42:1387–401. https://doi.org/10.1111/FFE.12994.
[87] Staykov A, Yamabe J, Somerday BP. Effect of hydrogen gas impurities on the hydrogen dissociation on iron surface. Int J Quant Chem 2014;114:626–35. https://doi.org/10.1002/QUA.24633.
[88] Somerday BP, Sofronis P, Nibur KA, San Marchi C, Kirchheim R. Elucidating the variables affecting accelerated fatigue crack growth of steels in hydrogen gas with low oxygen concentrations. Acta Mater 2013;61:6153–70. https://doi.org/10.1016/J.ACTAMAT.2013.07.001.
[89] Staykov A, Komoda R, Kubota M, Ginet P, Barbier F, Furtado J. Coadsorption of CO and H2 on an iron surface and its implication on the hydrogen embrittlement of iron. J Phys Chem C 2019;123:30265–73. https://doi.org/10.1021/ACS.JPCC.9B06927.
[90] Shang J, Chen W, Zheng J, Hua Z, Zhang L, Zhou C, et al. Enhanced hydrogen embrittlement of low-carbon steel to natural gas/hydrogen mixtures. Scr Mater 2020;189:67–71. https://doi.org/10.1016/J.SCRIPTAMAT.2020.08.011.
[91] Kim C, Kim W-S, Kho Y-T. The effects of hydrogen embrittlement by cathodic protection on the CTOD of buried natural gas pipeline. Met Mater Int 2002;8:197–202. https://doi.org/10.1007/BF03027018.
[92] Trasatti SP, Sivieri E, Mazza F. Susceptibility of a X80 steel to hydrogen embrittlement. Mater Corros 2005;56:111–7. https://doi.org/10.1002/maco.200403821.
[93] Alvarez JA, Gutierrez-Solana F, Cicero S. Environmental effect on pipeline steels: a fitness for service perspective. Fract Nano Eng Mater Struct 2006:611–2. https://doi.org/10.1007/1-4020-4972-2_303.
[94] Wang R. Effects of hydrogen on the fracture toughness of a X70 pipeline steel. Corrosion Sci 2009;51:2803–10. https://doi.org/10.1016/j.corsci.2009.07.013.
[95] Kyriakopoulou H, Karmiris-Obratański P, Tazedakis A, Daniolos N, Dourdounis E, Manolakos D, et al. Investigation of hydrogen embrittlement susceptibility and fracture toughness drop after in situ hydrogen cathodic charging for an X65 pipeline steel. Micromachines 2020;11:430. https://doi.org/10.3390/mi11040430.
[96] Xu K. Hydrogen embrittlement of carbon steels and their welds. In: Gaseous hydrog. Embrittlement mater. Energy technol. Elsevier; 2012. p. 526–61. https://doi.org/10.1533/9780857093899.3.526.
[97] Hagiwara N, Oguchi N. Fracture toughness of line pipe steels under cathodic protection using crack tip opening displacement tests. Corrosion 1999;55:503–11. https://doi.org/10.5006/1.3284013.
[98] Wang Y, Gong J, Jiang W. A quantitative description on fracture toughness of steels in hydrogen gas. Int J Hydrogen Energy 2013;38:12503–8. https://doi.org/10.1016/J.IJHYDENE.2013.07.033.
[99] Kim Y, Chao YJ, Pechersky MJ, Morgan MJ. On the effect of hydrogen on the fracture toughness of steel. Int J Fract 2005;134:339–47. https://doi.org/10.1007/S10704-005-1974-7. 1343 2005.
[100] Serebrinsky S, Carter EA, Ortiz M. A quantum-mechanically informed continuum model of hydrogen embrittlement. J Mech Phys Solids 2004;52:2403–30. https://doi.org/10.1016/J.JMPS.2004.02.010.
[101] Fu L, Fang H. Formation criterion of hydrogen-induced cracking in steel based on fracture mechanics. Metals 2018;8:940. https://doi.org/10.3390/met8110940.
[102] Huang S, Hui H. Predictive environmental hydrogen embrittlement on fracture toughness of commercial ferritic steels with hydrogen-modified fracture strain model. Int J Hydrogen Energy 2022;47:10777–87. https://doi.org/10.1016/j.ijhydene.2021.12.128.
[103] Huang S, Zhang Y, Yang C, Hu H. Fracture strain model for hydrogen embrittlement based on hydrogen enhanced localized plasticity mechanism. Int J Hydrogen Energy 2020;45:25541–54. https://doi.org/10.1016/J.IJHYDENE.2020.06.271.
[104] Olden V, Thaulow C, Johnsen R, Østby E, Berstad T. Influence of hydrogen from cathodic protection on the fracture susceptibility of 25%Cr duplex stainless steel – constant load SENT testing and FE-modelling using hydrogen influenced cohesive zone elements. Eng Fract Mech 2009;76:827–44. https://doi.org/10.1016/j.engfracmech.2008.11.011.
[105] Jemblie L, Olden V, Akselsen OM. A review of cohesive zone modelling as an approach for numerically assessing hydrogen embrittlement of steel structures. Philos Trans R Soc A Math Phys Eng Sci 2017;375. https://doi.org/10.1098/RSTA.2016.0411.
[106] Falkenberg R, Brocks W, Dietzel W, Scheider I. Modelling the effect of hydrogen on ductile tearing resistance of steels. Int J Mater Res 2010;101:989–96. https://doi.org/10.3139/146.110368/MACHINEREADABLECITATION/RIS.
[107] Moriconi C, Hénaff G, Halm D. Cohesive zone modeling of fatigue crack propagation assisted by gaseous hydrogen in metals. Int J Fatigue 2014;68:56–66. https://doi.org/10.1016/J.IJFATIGUE.2014.06.007.
[108] Brocks W, Falkenberg R, Scheider I. Coupling aspects in the simulation of hydrogen-induced stress-corrosion cracking. Procedia IUTAM 2012;3:11–24. https://doi.org/10.1016/J.PIUTAM.2012.03.002.
[109] Fassina P, Brunella MF, Lazzari L, Re G, Vergani L, Sciuccati A. Effect of hydrogen and low temperature on fatigue crack growth of pipeline steels. Eng Fract Mech 2013;103:10–25. https://doi.org/10.1016/J.ENGFRACMECH.2012.09.023.
[110] Nguyen TT, Heo HM, Park J, Nahm SH, Beak UB. Fracture properties and fatigue life assessment of API X70 pipeline steel under the effect of an environment containing hydrogen. J Mech Sci Technol 2021;354:1445–55. https://doi.org/10.1007/S12206-021-0310-0. 2021;35.

[111] Zhang S, Li J, An T, Zheng S, Yang K, Lv L, et al. Investigating the influence mechanism of hydrogen partial pressure on fracture toughness and fatigue life by in-situ hydrogen permeation. Int J Hydrogen Energy 2021;46:20621–9. https://doi.org/10.1016/J.IJHYDENE.2021.03.183.
[112] Wasim M, Djukic MB, Ngo TD. Influence of hydrogen-enhanced plasticity and decohesion mechanisms of hydrogen embrittlement on the fracture resistance of steel. Eng Fail Anal 2021;123:105312. https://doi.org/10.1016/J.ENGFAILANAL.2021.105312.
[113] Yamabe J, Yoshikawa M, Matsunaga H, Matsuoka S. Effects of hydrogen pressure, test frequency and test temperature on fatigue crack growth properties of low-carbon steel in gaseous hydrogen. In: Procedia struct. Integr., vol. 2. Elsevier B.V.; 2016. p. 525–32. https://doi.org/10.1016/j.prostr.2016.06.068.
[114] Shinko T, Hénaff G, Halm D, Benoit G, Bilotta G, Arzaghi M. Hydrogen-affected fatigue crack propagation at various loading frequencies and gaseous hydrogen pressures in commercially pure iron. Int J Fatigue 2019;121:197–207. https://doi.org/10.1016/J.IJFATIGUE.2018.12.009.
[115] Meng B, Gu C, Zhang L, Zhou C, Li X, Zhao Y, et al. Hydrogen effects on X80 pipeline steel in high-pressure natural gas/hydrogen mixtures. Int J Hydrogen Energy 2017;42:7404–12. https://doi.org/10.1016/j.ijhydene.2016.05.145.
[116] Amaro RL, White RM, Looney CP, Drexler ES, Slifka AJ. Development of a model for hydrogen-assisted fatigue crack growth of pipeline steel. J Press Vessel Technol Trans ASME 2018;140. https://doi.org/10.1115/1.4038824/383751.
[117] San Marchi C, Somerday BP, Nibur KA. Development of methods for evaluating hydrogen compatibility and suitability. Int J Hydrogen Energy 2014;39:20434–9. https://doi.org/10.1016/j.ijhydene.2014.03.234.
[118] Asme B31G. 12-2019 hydrogen piping and pipelines ASME code for pressure piping. American Society of Mechanical Engineers; 2019.
[119] Cga G-5. 6-2005 R2013 hydrogen pipeline systems. In: Reaffirmed 2013. Compressed gas association. 1st ed. the European Industrial Gases Association; 2013.
[120] Yanagisawa Y, Yoru W, Ohmi T, Yokobori AT. Hydrogen-assisted cracking threshold of high-strength low-alloy steel. In: Mater. Fabr., 6B. American Society of Mechanical Engineers; 2015. https://doi.org/10.1115/PVP2015-45337.
[121] Akhi AH, Dhar AS. Fracture parameters for buried cast iron pipes subjected to internal surface corrosions and cracks. J Pipeline Sci Eng 2021;1:187–97. https://doi.org/10.1016/J.JPSE.2021.04.001.
[122] Wong CK, Wan RG, Wong RCK. Performance of buried pipes in moving slopes under axial loading – evaluation tools. J Pipeline Sci Eng 2021;1:167–75. https://doi.org/10.1016/J.JPSE.2021.05.005.
[123] Dadfarnia M, Sofronis P, Brouwer J, Sosa S. Assessment of resistance to fatigue crack growth of natural gas line pipe steels carrying gas mixed with hydrogen. Int J Hydrogen Energy 2019;44:10808–22. https://doi.org/10.1016/J.IJHYDENE.2019.02.216.
[124] Drexler ES, Amaro RL, Slifka AJ, Bradley PE, Lauria DS. Operating hydrogen gas transmission pipelines at pressures above 21 MPa, vol. 140. J Press Vessel Technol Trans ASME; 2018. https://doi.org/10.1115/1.4041689.
[125] Park GT, Koh SU, Jung HG, Kim KY. Effect of microstructure on the hydrogen trapping efficiency and hydrogen induced cracking of linepipe steel. Corrosion Sci 2008;50:1865–71. https://doi.org/10.1016/J.CORSCI.2008.03.007.
[126] Stalheim D, Boggess T, Marchi CS, Jansto S, Somerday B, Muralidharan G, et al. Microstructure and mechanical property performance of commercial grade API pipeline steels in high pressure gaseous hydrogen. Proc Bienn Int Pipeline Conf IPC 2011;2:529–37. https://doi.org/10.1115/IPC2010-31301.
[127] Zhang T, Zhao W, Deng Q, Jiang W, Wang Y, Wang Y, et al. Effect of microstructure inhomogeneity on hydrogen embrittlement susceptibility of X80 welding HAZ under pressurized gaseous hydrogen. Int J Hydrogen Energy 2017;42:25102–13. https://doi.org/10.1016/J.IJHYDENE.2017.08.081.